Strål
säkerhets
myndigheten
Swedish Radiation Safety Authority

Authors:
Weilin Zang
Jens Gunnars
Pingsha Dong
Jeong K. Hong

Research

2009:15

Improvement and Validation of Weld Residual Stress Modelling Procedure

Report number: 2009:15 **ISSN:** 2000-0456
Available at www.stralsakerhetsmyndigheten.se

Title: Improvement and Validation of Weld Residual Stress Modelling Procedure.
Report number: 2009:15
Authors: Weilin Zang[1)], Jens Gunnars[1)], Pingsha Dong[2)] and Jeong K. Hong[2)]
[1)]Inspecta Technology AB, Stockholm, Sweden. [2)]Center for Welded Structures Research, Battelle, Columbus, Ohio
Date: June 2009

Background

Weld residual stresses have a large influence on the behavior of cracks growing under normal operation loads and on the leakage-flow from a through-wall crack. Accurate prediction of these events is important in order to arrive at proper conclusions when assessing detected flaws, for inspection planning and for assessment of leak-before-break margins. Therefore, it is very important to have verified procedures to estimate weld residual stresses (WRS). During the latest years, there has been a strong development in both analytical procedures to numerically determine WRS and experimental measurements of WRS. The present report is the result of an effort to acquire and to develop the latest research results in the field of WRS.

Objectives of the project

The principal objective of the project is to use the latest research results of determining WRS in piping components and verify such procedures against experimental measurements.

Results

The major changes applied in the new weld residual stress modelling procedure are:

- Improved procedure for heat source calibration based on use of analytical solutions.
- Use of an isotropic hardening model where mixed hardening data is not available.
- Use of an annealing model for improved simulation of strain relaxation in re-heated material.

The new modelling procedure is demonstrated to capture the main characteristics of the through-thickness stress distributions by validation against experimental measurements. Three austenitic stainless steel butt-welds cases are analysed, covering a large range of pipe geometries. From the cases it is evident that there can be large differences between the residual stresses predicted using the new procedure, and earlier recommendations.

Effects on SSM

The results of this project will be used by SSM in safety assessments of welded components with cracks.

Project information

Project leader at SSM: Björn Brickstad
Project number: 14.42-200542009, SSM 2008/77
Project Organisation: Inspecta Technology AB has managed the project with Dr Jens Gunnars as the project manager. Center for Welded Structures Research, Battelle in Columbus, Ohio has been used as subcontractor to Inspecta Technology AB for certain project tasks.

Contents

1 SUMMARY

The objective of this work is to identify and evaluate improvements for the residual stress modelling procedure currently used in Sweden. There is a growing demand to eliminate any unnecessary conservatism involved in residual stress assumptions. The study was focused on the development and validation of an improved weld residual stress modelling procedure, by taking advantage of the recent advances in residual stress modelling and stress measurement techniques.

The major changes applied in the new weld residual stress modelling procedure are:

- Improved procedure for heat source calibration based on use of analytical solutions.
- Use of an isotropic hardening model where mixed hardening data is not available.
- Use of an annealing model for improved simulation of strain relaxation in re-heated material.

The new modelling procedure is demonstrated to capture the main characteristics of the through-thickness stress distributions by validation to experimental measurements. Three austenitic stainless steel butt-welds cases are analysed, covering a large range of pipe geometries. From the cases it is evident that there can be large differences between the residual stresses predicted using the new procedure, and the earlier procedure or handbook recommendations. Previously recommended profiles could give misleading fracture assessment results. The stress profiles according to the new procedure agree well with the measured data. If data is available then a mixed hardening model should be used.

2 INTRODUCTION

Stress corrosion cracking (SCC) is a damage mechanism that has to be accounted for in performing structural integrity assessments and inspection planning of stainless steel components in Swedish nuclear plants [1-3]. In an unfavourable environment, tensile stresses create a necessary condition for stress-corrosion cracking to take place. Welding-induced residual stresses have a significant contribution to both the initiation and the subsequent growth of SCC in welded components. Weld residual stresses may also influence the final fracture behaviour. However, in ductile steels in nuclear components the effect of secondary loads is sometimes limited and not decisive for the critical and tolerable crack sizes.

Accurate prediction of weld residual stress fields has a significant influence on the prediction of stress corrosion crack growth, and is decisive for proper conclusions on inspection intervals. Inaccurate estimation of residual stress fields may also influence conclusions about leak-before-break. Consequently it is important to have reliable estimates of weld residual stress distributions, in order to avoid non-conservative or misleading conclusions, and to ensure effective measures for safe operation of nuclear power plants.

Through-wall residual stress distributions can exhibit rather different forms at a weld, depending on factors such as: pipe thickness, number of passes, weld geometry, deposition sequence, pipe radius to thickness ratio, global restraints, material properties, weld method, interpass temperature, and heat input [4-8]. A reliable finite element residual stress modelling method must be able to capture the correct residual stress distribution under given pipe and welding conditions. Earlier efforts in Sweden have established a residual stress modelling procedure [6] and a series of recommended residual stress solutions [7-8, 3]. These results have been widely used for meeting the needs in performing assessment of cracks and planning inspections for Swedish nuclear plants. However, further developments and new conclusions in residual stress modelling techniques have emerged since the development of this procedure [4-5, 9-12]. Recent reviews [4, 13] of recommended residual stress fields calculated by different analysis procedures and organisations, shows that residual stress profiles differ very much in many cases. Furthermore, the possibility to compare to measured data has improved since detailed residual stress measurement data has become available through different international programs [13-15]. This new information gives possibilities for validation and improvement of the existing residual stress modelling procedure [6]. Recent advances in residual stress measurement techniques such as deep hole drilling [16, 17], high energy synchrotron X-ray diffraction [18, 19], neutron diffraction [20-22], and surface contouring [23-25] will further improve the capabilities to measure through thickness residual stress distributions accurately, and some methods even offer a potential for determining full 3D stress tensor results deep within components.

The objective of this work is to identify and propose improvements to the existing residual stress modelling procedure currently used in Sweden [6-8, 3], by taking advantage of the recent developments. The procedure will be validated to a set of existing measurement results. The project was set up as a collaboration effort between Inspecta and Battelle, with the following objectives:

1) Identify areas for improvement in the existing residual stress modelling procedure
2) Develop improved residual stress estimation procedures by performing technology transfer
3) Perform case studies on a selected set of pipe geometries, representative for Swedish nuclear plants. This is done in order to evaluate and validate the effectiveness of the improved modelling procedures, by comparisons to well documented measured residual stress fields.

4) Investigate and recommend how to evaluate and treat residual stress when performing fracture mechanics analysis of welded components, to improve accuracy and decrease any excessive conservatism involved in earlier procedures used.

The project was carried out in two phases. Phase 1 focused on improvement and validation of the weld residual stress modelling procedure, and included step 1) - 3) above. This phase also involved a one-week long training at Battelle on the mechanics of residual stresses in welded joints and associated modelling procedures. Available residual stress measurement data relevant to nuclear piping components were collected for validating the residual stress modelling procedure. A series of residual stress analyses were performed for components on which the measurement data was available, by using the recommended residual stress modelling procedures established during the project. This report provides a detailed documentation for Phase 1. The work performed during Phase 2, which was focused upon fracture mechanics treatment procedures of the residual stress distributions, is documented in a separate report.

3 RESIDUAL STRESS MODELLING PROCEDURE

3.1 The previous procedure used by Inspecta

The previous weld residual stress modelling procedure used at Inspecta (and formerly at DNV and SAQ) was based on the work documented in [6-8]. The recommended stress profiles in the handbook [3] are based on this procedure. The residual stress modelling procedure involves sequentially coupled heat-conduction-based thermal analysis of the welding heat flow and a subsequent incremental thermo-plastic analysis which is dependent on the predicted temperature history [6]. Areas of improvement concerning this procedure are identified and discussed below.

Axi-symmetric assumptions are normally used for modelling multi-pass welds in piping components, in order to simplify the analysis procedure and achieve a realistic analysis time. This implies a simultaneous weld deposition along the entire pipe circumference, and the heat loss in the welding travel direction is ignored. As discussed in [4], this may result in overheating effects, depending on how the linear heat input from the welding parameters is used. Careful calibration is always needed and improvement of the principles for this is identified as an important improvement area.

In the previous procedure [6] it was assumed that the material has a kinematic strain-hardening behaviour. This assumption was consistent with most of the modelling published in the literature at that time. At that time few reliable experimental measurements of residual stress fields existed and a general recommendation was to use kinematic hardening. However recent results indicate that the through thickness residual stress profiles are better captured using an isotropic hardening model. If cyclic stress-strain data would be available, then a mixed isotropic-kinematic hardening model could be used. This type of data is however rare.

Weld pass deposition is simulated by the addition of new molten material using “element remove/include” technique (inactive elements). Newly activated elements achieve zero strain by this technique. In the previous procedure re-heated weld and base metal adjacent to the new bead did not, however, achieve zero plastic strain (unless a general user subroutine was programmed). Due to the lack of an “annealing” procedure, i.e. simulation of zero strain in hot or re-melted metal, artificial strain accumulation existed which affected the final residual stress results. Anneal modelling capabilities only recently became available in ABAQUS [26]. The anneal temperature can simulate rapid strain relaxation at high temperatures, due to microstructural processes in material re-heated to high temperature or re-melted.

3.2 The new updated procedure

The previous procedure described in [6-8] is modified, by taking advantage of the most recent developments in finite element residual stress modelling techniques as discussed in [4-5, 9-14]. The new updated residual stress modelling procedure that has been established during this project is described below. Modelling capabilities that are only recently available in ABAQUS are incorporated in the new procedure. Validation has been performed using Battelle's proprietary modelling tools, which are capable of simulating the detailed residual stress development [4]. Validation has also been done by comparison with well-documented residual stress measurement data, as reported in Section 4.

3.2.1 Transient thermal analysis

The weld residual stress modelling procedure starts with a transient thermal analysis of the welding heat flow. Addition of new molten weld material is modelled using the element-include technique (inactive elements). If necessary, the quiet element technique (a low stiffness deforming mesh) could be used in order to achieve a good deformation and adaptation of the element mesh for the non-added beads. The transient thermal history provides input for a subsequent incremental thermo-plastic analysis. Similar to the earlier procedure, the thermal material properties are temperature-dependent. A heat transfer boundary condition is applied at all free surfaces of the component. The free boundary is altered in space as new weld passes are added. The boundary condition is described by a resulting heat transfer coefficient α_h (approximating both convection and radiation), given by [6]:

$$\begin{aligned} &\alpha_h = 0.0668 \cdot T \qquad W/\left(m^2\ ^\circ C\right) \qquad 20^\circ C \le T \le 500^\circ C \\ &\alpha_h = 0.231 \cdot T - 82.1 \quad W/\left(m^2\ ^\circ C\right) \qquad T > 500^\circ C \end{aligned} \tag{3.1}$$

The heat source model for a specific welding method needs to be calibrated by different methods, through the use of theoretical models and experimental data. From etched cross sections of a weld by the actual welding process and in the actual material, metallurgical information can help to identify what temperatures there have been at different distances from the melted material in the weld pool. Cross sections also give information on typical shape of the weld pool and the section area of the bead fusion zoon resulting from the welding process used and different sets of weld parameters. Information for the heat source modelling can also be obtained from temperature measurements very close to weld passes by thermal gages, and by thermal imaging methods for assessing the length of the weld pool.

The weld pass heat input per unit run length Q can be calculated from welding process parameters as

$$Q = \eta \frac{IU}{v} \tag{3.2}$$

where I is the current, U is voltage, η is the electrical heat input efficiency per welding process, and v is weld travel speed. The heat input efficiency for different welding processes is typically 0.95 for SAW, 0.8 for MMA (or SMAW), and 0.6 for TIG.

When a 2D approximation is used, e.g. rotational symmetry for simulating pipe girth welding, the assumed conditions in the model resemble those corresponding to a simultaneous deposition of the weld pass along the entire weld length. The heat conduction in the welding travel direction is by

definition ignored in a 2D model, and the heat input to the structure is exaggerated. This implies an extra need for calibration of the heat source model in 2D models in order to avoid overheating from the simulation.

A typical heat source model for arc welding process as MMA, SAW and TIG is illustrated by Figure 3.1. The figure shows the temperature in the centre of a newly added weld bead. The temperature is rapidly rising to the melting temperature T_{melt} and the filler material holds that temperature under the period τ_2^i, before it starts to cool down and solidify, since the weld pool is moving on. For these welding processes the dominating part of the melted material is new added filler material, and the majority of Q is consumed in the new filler material. The time τ_1^i is short compared to τ_2^i. The material continue to cool down and has the temperature $T_{intpass}$ at the instant τ_3^i when the next adjacent weld pass is made. The temperature $T_{intpass}$ is the inter-pass temperature, and is often about 150 °C. The time τ_3^i is long compared to τ_2^i.

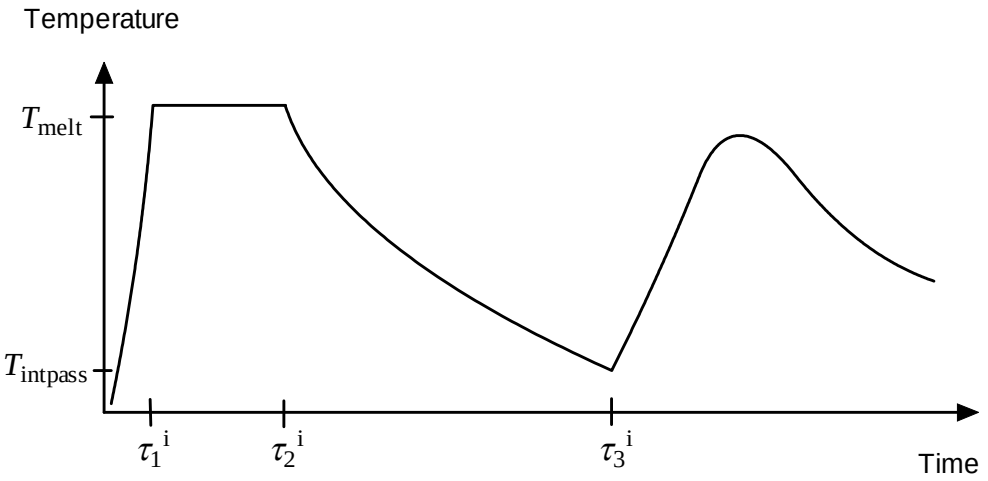

Figure 3.1. Temperature transient in newly deposited weld pass a function of time.

The steps in the transient heat condition analysis of a weld ars described below. A two-dimensional model is considered, and a description of a procedure for the heat source calibration for a 2D axi-symmetric model is included. Any specified pre-heating is modelled by a corresponding initial temperature step for the pipe. The thermal modelling of a new weld pass involves the following steps:

1) A new weld pass to be deposited receives a temperature slightly higher than the melting temperature T_{melt}. The addition of molten weld material is modelled using the element-include technique, i.e. a group of elements representing the new weld bead is activated. The size of the fusion zone/bead is related to the weld bead cross sectional area achieved from metallographic macro cross sections of the weld for the actual set of welding parameters.

2) A transient heat conduction analysis is then performed to simulate the subsequent heat transfer process after the new weld bead is introduced. The weld bead has the temperature T_{melt} under the time period τ_2^i, before it starts to cool down and solidify as the weld pool passes by. For calibration of the heat source, the time τ_2^i is determined based on the following considerations:

- The time τ_2^i is determined based on the use of analytical 3D moving heat source solution [27-31, 22]. The influence of the pipe thickness is accounted for by using a solution developed from two mirrored travelling heat sources.
- The heat affected zone (HAZ) size is determined by the 3D analytical solution for a given pipe thickness, the thermal diffusivity of the material, and the linear heat input Q and the travelling speed v for the actual weld pass.
- The HAZ size is defined by the distance between the fusion line and nearest position that reaches to the first phase transformation, i.e. temperature A_{c1} for ferritic steels and about $800C^o$ for stainless steels [14].
- For the 2D model, the next step is to calibrate the time τ_2^i by analytical solution, in order to compensate for the missing heat loss in the welding direction (the hoop direction), compared to a 3D travelling heat source.

The effectiveness of this calibration method has been evaluated and verified by detailed finite element calculations performed by Battelle, as documented in [14].

3) The inter-pass time τ_3^i is adjusted to receive the prescribed overall inter-pass temperature T_{intpass} before the next weld pass is activated

4) The procedure is repeated until all weld beads are added, and then the entire model reaches steady-state room temperature conditions.

5) Any post-weld heat treatment is modelled, and any other thermal loading that may redistribute the residual stress field is modelled.

3.2.2 Thermo-elastic-plastic mechanical analysis

Once the temperature history is generated using the procedure described above, stresses and strains are calculated by performing a thermo-elastic-plastic analysis. Small strain theory is normally used. The analysis follows the given temperature history on a pass per pass basis, until all weld passes are simulated.

The mechanical properties are temperature-dependent. Incremental plasticity is used with the von Mises yield criterion and associated flow rule. The material hardening law is assumed to be isotropic hardening. A bilinear stress-strain relation is applied, details of which are available in Appendix 1. The experience from recent comparisons to measured weld residual stress fields indicate that the through thickness stress profiles are better captured using an isotropic hardening model [4, 13]. If detailed cyclic stress-strain material properties are available, then a mixed isotropic-kinematic hardening model could be used (an expanding and translating yield surface). There are arguments claiming that the effect of the isotropic hardening part dominates over the kinematic part, which would support the isotropic approximation.

The multi-pass weld is modelled by activating the elements belonging to the current pass at a proper time, consistent with the transient heat flow simulation procedure. In the earlier procedure, the "element include" technique in ABAQUS was utilized for assuring zero plastic strains in new activated elements. However, by this modelling unrealistic plastic strains did accumulate in areas close to the fusion line and in HAZ, which affected the final residual stress results. Weld and base material

adjacent to a new weld bead will reach high temperatures or even re-melt, and the strain relaxation, and the new strain free temperature, in these regions were not modelled. In order to simulate this effect, the new annealing capability in ABAQUS is now utilized for simulation of strain relaxation in hot and re-melted metal.

Few experimental results are reported about the exact extent to which weld strains are annealed, or the extent of strain relaxation in re-heated or re-melted material. Local stress-strain curves in as-welded material are presented in [15] and [35] and the measured local yield stress in as-welded filler material and in HAZ corresponds to 5 - 10% strain hardening of the base/virgin material. This could indicate some degree of strain relaxation, since simulations often generate more strain than that.

Annealing and strain relaxation arises at high temperatures, due to different microstructural processes as recrystallization and rapid creep. Conventional annealing is performed using long hold times (hours) and starts with temperatures from 1/3 of the melting temperature. However, for the rapid temperature transient during welding the amount of annealing in different regions, and the dominating process, is not clarified. It is expected that annealing effects are only seen in regions of much higher temperatures than 1/3 of the melting temperature, because of the short effective hold time.

By utilizing the anneal temperature capability in ABAQUS it is possible to prescribe a temperature above which strain-free conditions are assumed, in order to reset accumulated plastic strains and the hardening. The anneal temperature can simulate rapid strain relaxation at high temperatures, or in re-melted material. Data for the rate of recrystallization or creep at high temperatures is however rare, but it has been argued for the use of an “anneal temperature“ in the range 900 - 1200 °C, depending on the estimated effective time at high temperatures and the dominating process for strain relaxations. In general the assumption of a high annealing temperature results in higher stresses, and generally we assume an annealing temperature of 1200 °C in the new modelling procedure. In order to establish actual annealing temperature to use for different materials further work is required. Sensitivity analyses are performed in section 5. The annealing modelling was also investigated by some comparisons to the results from the Battelle’s proprietary weld material model (“UMAM”) which is capable of simulating annealing effects as a function of temperature.

Boundary conditions resembling the fixing conditions used (and possibly altered) during the welding are applied to the model. Any post-weld heat treatment and other mechanical loading that may redistribute the residual stress field is modelled.

4 SIMULATIONS AND VALIDATION TO MEASURED RESULTS

The new weld residual stress modelling procedure described in Section 3.2 was applied to a set of cases were residual stress measurement results are available from the literature for well documented weld mock-ups. The purpose was to validate proposed modified procedure to experimental measurements for future improved prediction of the weld residual stresses.

Three different pipe welds are simulated. Basic data for the three cases investigated are summarized in Table 1. Axi-symmetric modelling was used in all cases. The welding inter-pass temperature was assumed to be room temperature, which will tend to over-estimate residual stresses if the actual in-pass temperature were higher. The simulations were performed assuming general data for austenitic stanless steel, according to [6, 7] – see Appendix A. Isotropic hardening behaviour was assumed in all cases. The annealing temperature was set to 1200°C.

Sensitivity studies with respect to the assumed hardening model and annealing temperature are presented in Section 5 for the case 2 weld. The residual stress profile has been measurement in detail for these cases by neutron diffraction, deep-hole-drilling, and surface-hole drilling techniques, and documentation of the cases are found in [13, 32, 33].

All presented results are for 20ºC.

Table 1: Case definition.

Case No.	**Name**	**Pipe thickness t [mm]**	**Pipe radius to thickness ratio R_{in}/t**	**Groove type**	**Number of passes**	**Weld type**	**Heat input * [kJ/mm]**	**Weld speed * [mm/s]**	**Material (parent/weld)**
1	Weld C	15.9	25	X	2 + 4	TIG SAW	0.6 2.0	3 6	316L/316L
2	SP19	19	10.5	V	15 (*)	MMA	1.2	-	316H/316L
3	S5VOR	65	2.8	V	45	MMA	2.4	-	316H/316L

(*) Data not fully clear from the mock-up manufacturing information available.

4.1 Case 1 – Thin-walled pipe

A butt-weld in a thin-walled pipe having R_{in}/t = 25 is analysed, were R_{in} is the inner radius of the pipe and t is the pipe thickness. The geometry of the weld and the finite element mesh near the weld area are shown in Fig. 4.1. Axial symmetry is assumed. The length of the modelled pipe is larger than $3\sqrt{(Rt)}$ in order to avoid influence from the support, as discussed in [9]. The mesh design provides three straight line paths for evaluation of the residual stress results, denoted CL, HAZ, and HAZ_0, as shown in Fig. 4.1.

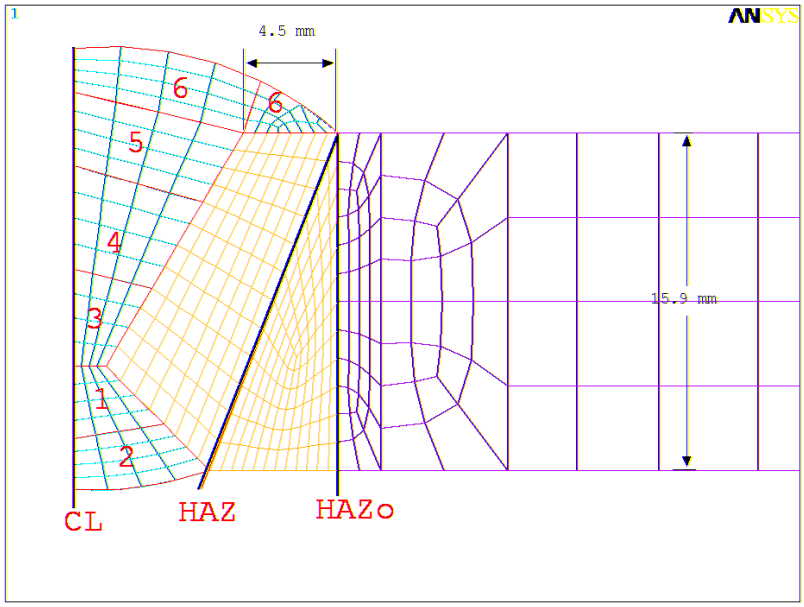

Figure 4.1: Geometry, sequence of welding and finite element mesh for Case 1.

After the transient heat flow analysis was completed for the six-pass welding as shown in Fig. 4.1, one check on the heat flow solution is examination of the peak temperature experienced in the model. Fig. 4.2 shows the peak temperature experienced during welding, enveloped over all weld passes. The resulting final fusion zone is indicated by the region with temperature above 1500 °C. The heat affected zone (HAZ) is outlined approximately by the temperature interval between about 700 °C and 1500 °C.

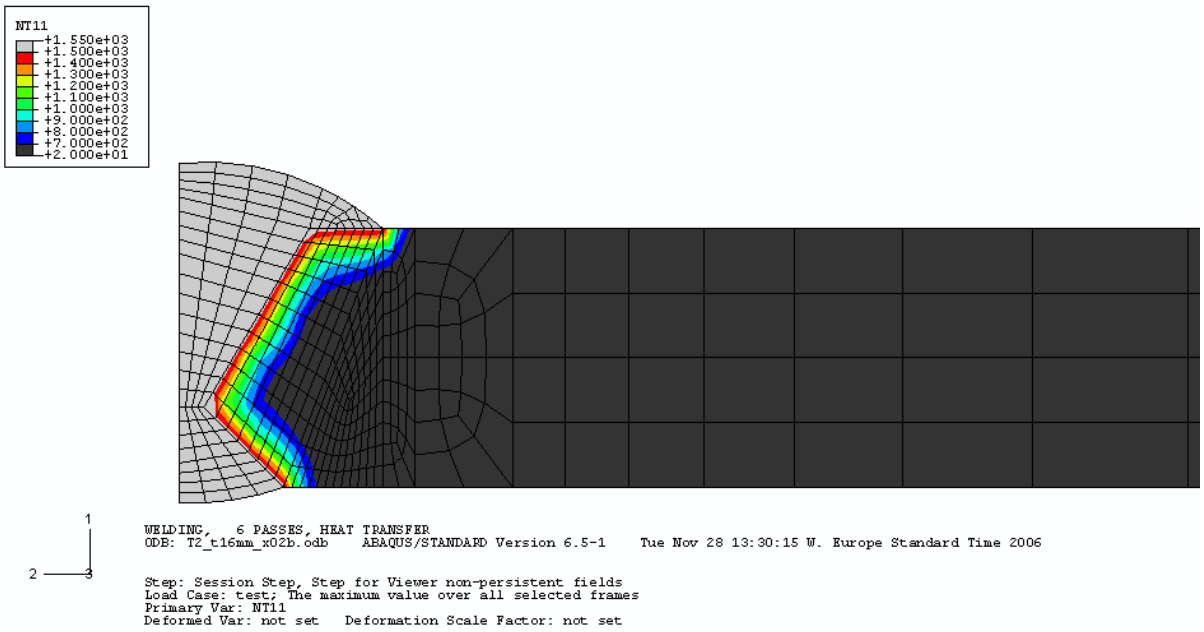

Figure 4.2: Fusion zone and HAZ. Maximum temperature experienced during welding. The locations with a maximum temperature exceeding 1500 °C are plotted with gray colour and the locations with a maximum temperature lower than 700 °C are shown with black colour.

The final residual stress distributions at 20°C (room temperature) are shown in Fig. 4.3 for the axial residual stress component and in Fig. 4.4 for the hoop stress component. The axial residual stress distribution in Fig. 4.3 is dominated by a through-wall bending feature characterized by an axial compression area on the outer diameter (OD) side and tension on the inner diameter (ID). The hoop residual stresses are dominated by overall tension within the weld zone, consistent with the residual stress distributions in similar pipe girth welds (in terms of *R/t* ratio and heat input) documented in [4].

This particular stainless steel pipe geometry and welding conditions (Fig. 4.1) have been documented in a publication by Bouchard [13], with detailed experimental residual stress measurement results from neutron diffraction (ND), deep hole drilling (DHD), surface hole drilling (SH), and block removal splitting and layering (BRSL) techniques.

In order to compare the predictions achieved using the new modelling procedure with the available measured stress data, the residual stress distributions along the three pre-defined paths in Fig. 4.1 are plotted with the measurement data reported in [13] in Figs. 4.5-4.7. The neutron diffraction measurements were taken 12mm from the weld centreline [38].

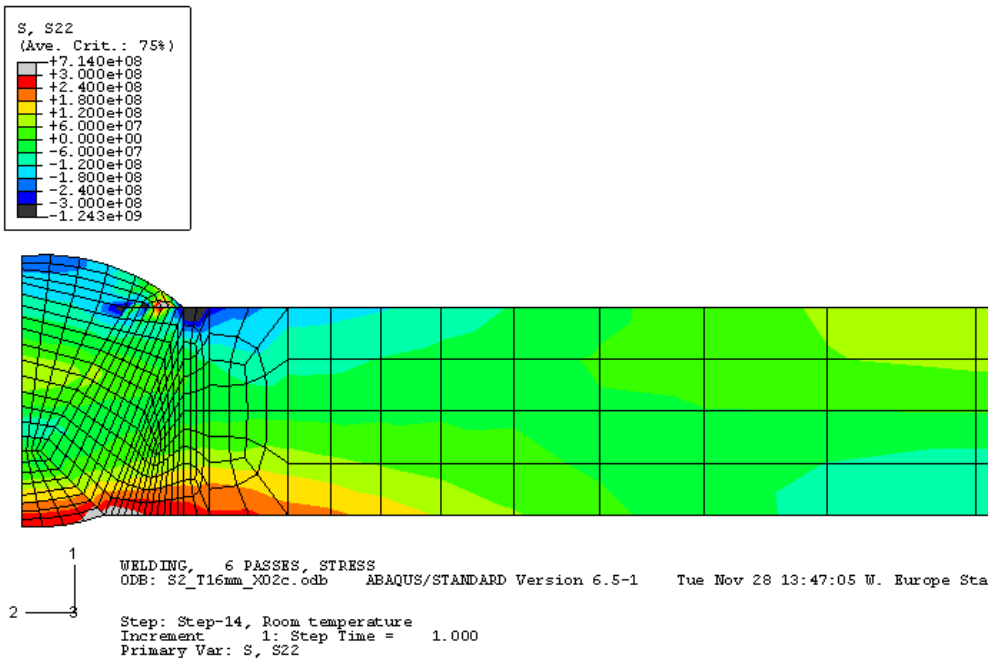

Figure 4.3: Axial residual stress for the thin-walled case 1 weld at 20 °C (unit Pa).

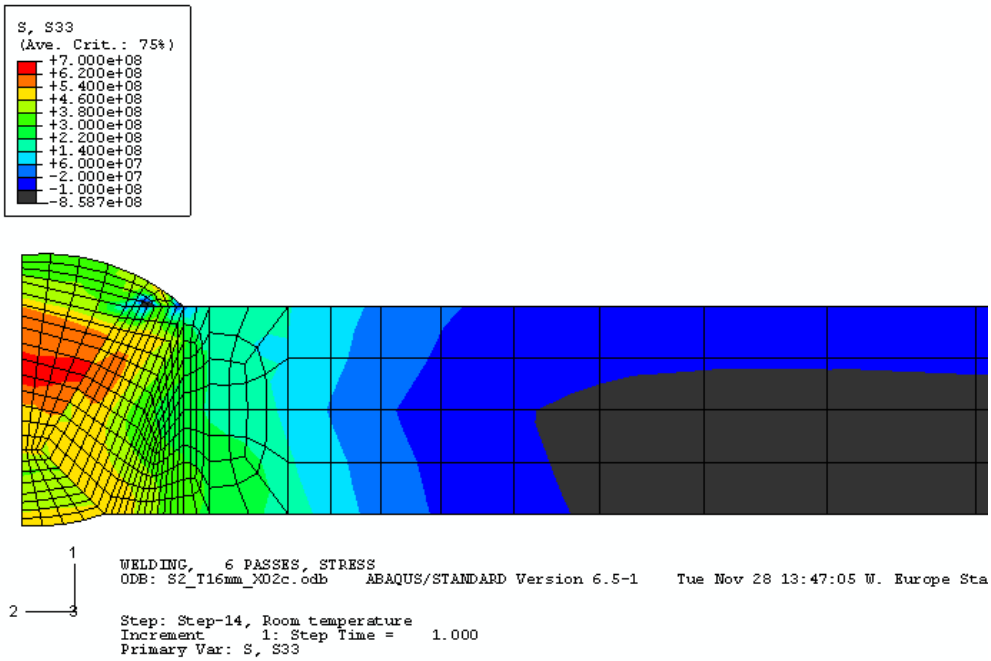

Figure 4.4: Hoop residual stress for the thin-walled case 1 weld at 20 °C (unit Pa).

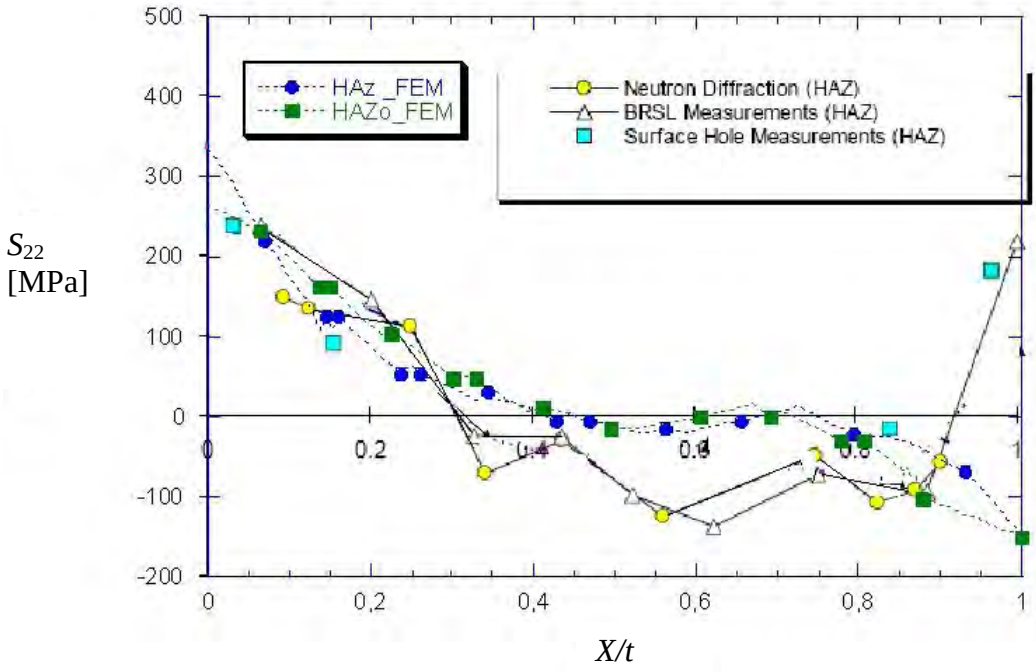

Figure 4.5: Case 1. Comparison of the predicted and measured axial residual stress (S_{22}) at 20 °C along the two HAZ paths shown in Fig. 4.1 (X/t = 0 corresponds to the ID surface).

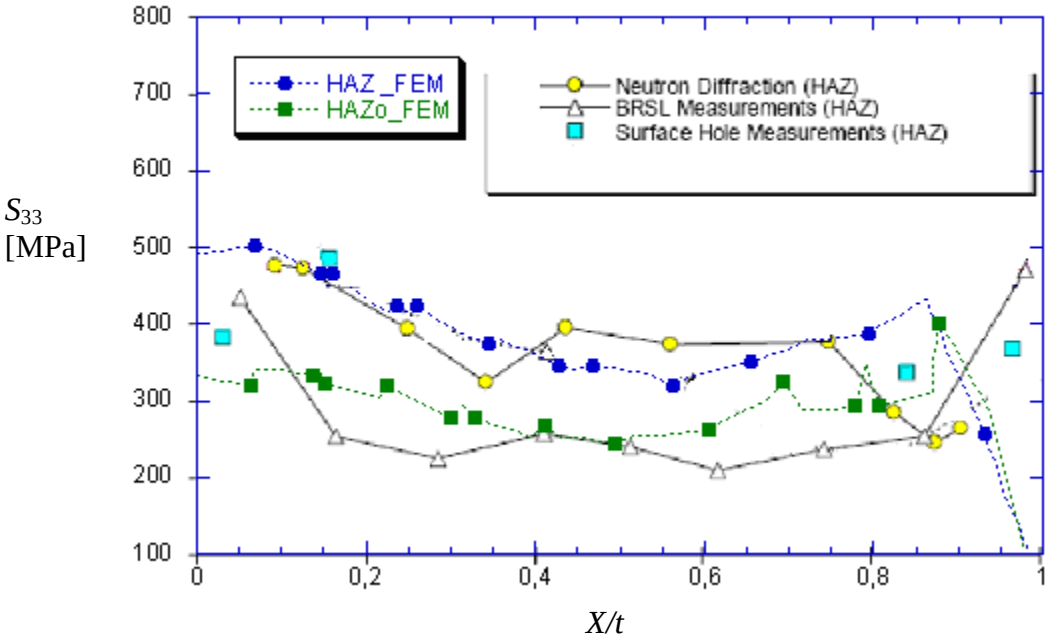

Figure 4.6: Case 1. Comparison of the predicted and measured hoop residual stress (S_{33}) at 20 °C along the two HAZ paths shown in Fig. 4.1 (X/t = 0 corresponds to ID surface).

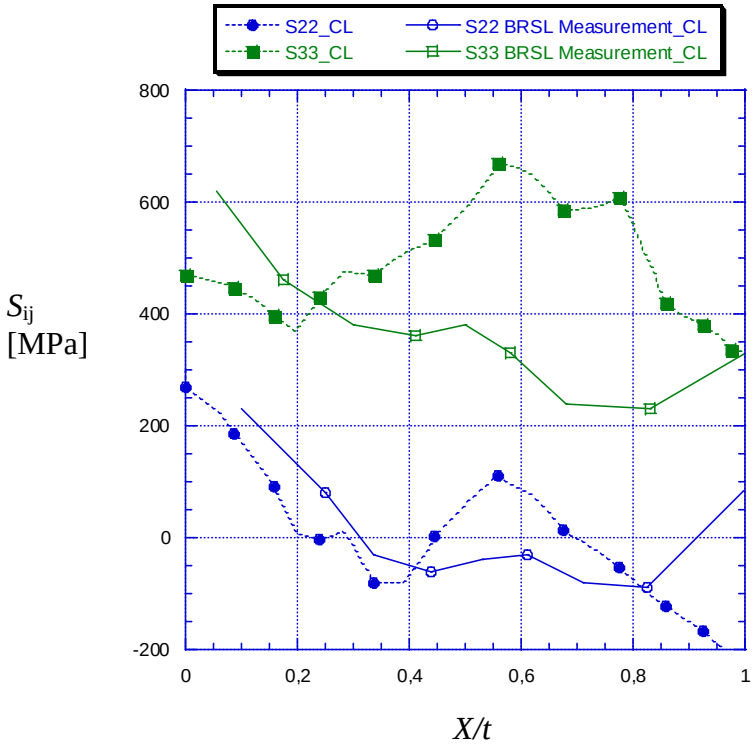

Figure 4.7: Case 1. Comparison of the predicted and measured residual stress at 20 °C along the weld centerline (CL in Fig. 4.1).

Measurements will always give a mean average value of the stress in a gauge volume in the material, and with some uncertainty with respect to the distance from the fusion line, see discussion in [22]. Considering this, it is reasonable for the comparison to be based on the average from the two evaluation paths in HAZ. The measurement data compared to in Figs. 4.5-4.7 were taken from an actual weld mock up and reflect measurements along a given path from the actual three dimensional pipe. As discussed in [34], the residual stress field in a multi-pass pipe butt-weld has a clearly-defined periodic variation along the pipe circumference, in addition to weld pass start and stop effects. In view of this and the fact that axisymmetric assumptions were used in the present analysis, the agreement between the predictions and measurements is rather reasonable.

4.2 Case 2 – Intermediate pipe

As the second case a medium thick-walled pipe having R_{in}/t = 10.5 was analysed. The geometry, the sequence of the weld passes, and the finite element mesh is shown in Fig. 4.8. Five through-wall paths selected for evaluation of the through-wall residual stress distributions are also shown in Fig. 4.8. The pipe geometry is given in Table 1. Detailed information on the weld mock-up fabrication and welding process parameters were taken from [13] and [32].

The peak temperature experienced during welding is shown in Fig. 4.9. The fusion zone for the 15-pass weld is indicated by a temperature exceeding 1500 °C. The HAZ is indicated by temperatures ranging from 700 °C to the fusion line (1500 °C).

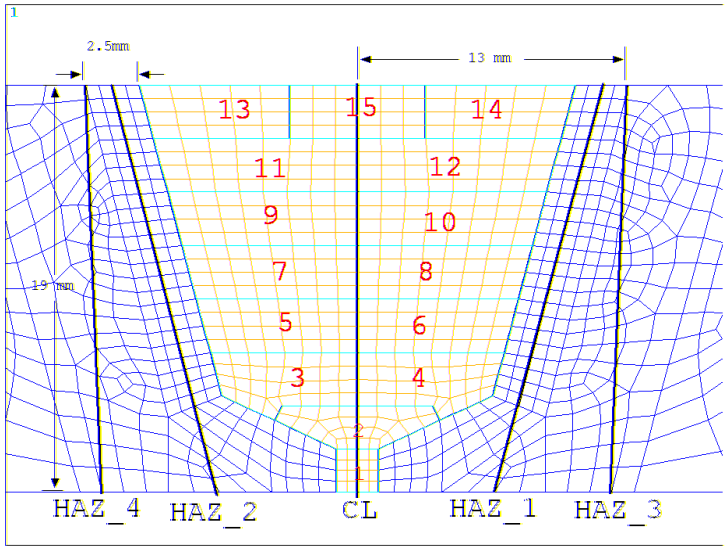

Figure 4.8: Geometry, definition of sequence of welding and finite element mesh for Case 2.

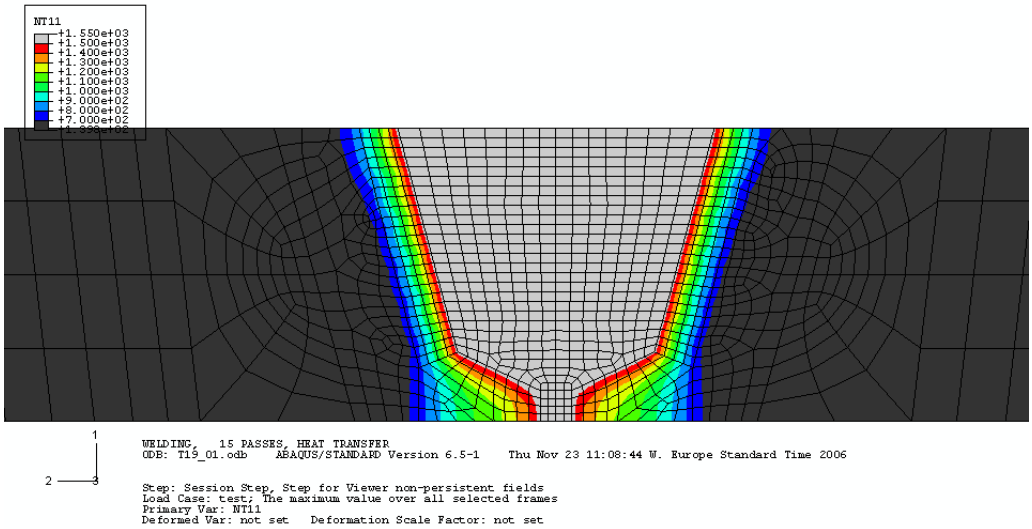

Figure 4.9: Fusion zone and HAZ. Maximum temperature experienced during the welding. The locations with a maximum temperature exceeding 1500 °C are plotted with gray colour and the locations with a maximum temperature lower than 700 °C are shown with black colour.

The predicted axial and hoop residual stress distributions are shown in Figs. 4.10-4.11. Comparing with the thin-wall pipe case (Case 1) in Fig. 4.3, the axial residual stress distribution for Case 2 (Fig. 4.10) differs in that the through-thickness distribution in and around the weld area no longer displays a clearly defined through-thickness bending feature, although the linear heat inputs between the two cases are similar. This difference clearly suggests that pipe R_{in}/t ratio and thickness compared to bead size has a significant effect on residual stress distributions in addition to linear heat input, as discussed in [4, 5]. As a result, the hoop residual stress distribution for Case 2 (Fig. 4.11) becomes noticeably more localized than that for Case 1. Detailed discussions on the mechanisms dominating such a transition in through-thickness distribution characteristics were given recently in [5].

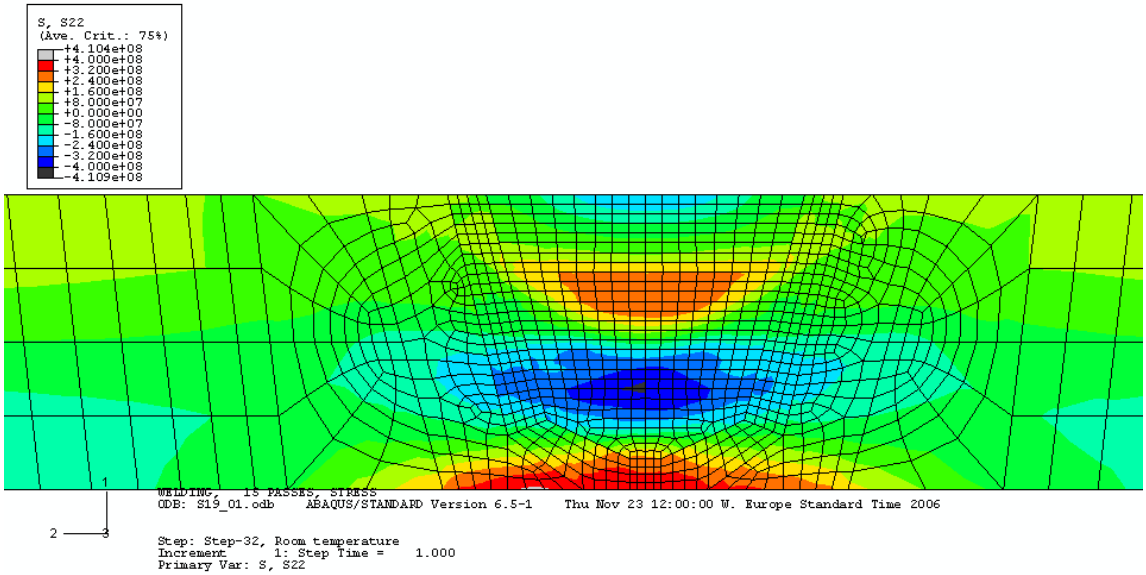

Figure 4.10: Axial residual stress for the medium thick-walled case 2 weld at 20 °C (unit Pa).

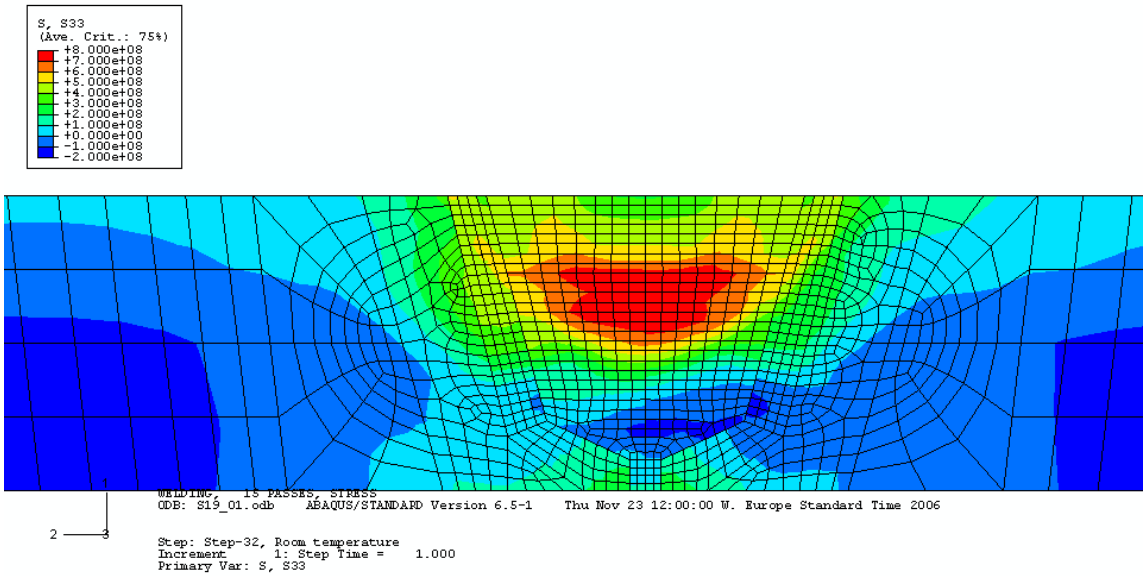

Figure 4.11: Hoop residual stress for the medium thick-walled case 2 weld at 20 °C (unit Pa).

The predicted residual stress distributions along various HAZ paths in Fig. 4.8 are compared with neutron diffraction measurement data documented in [13, 32], as shown in Figs. 4.12-13. In this case the neutron diffraction measurements were taken 14mm from the weld centreline. Again, a reasonably good agreement is seen, considering approximations and also measurement uncertainties. Fig. 4.14 shows the predicted axial and hoop residual stresses along the weld centreline CL (see Fig. 4.8), on which there were no experimental measurement data available for this particular case.

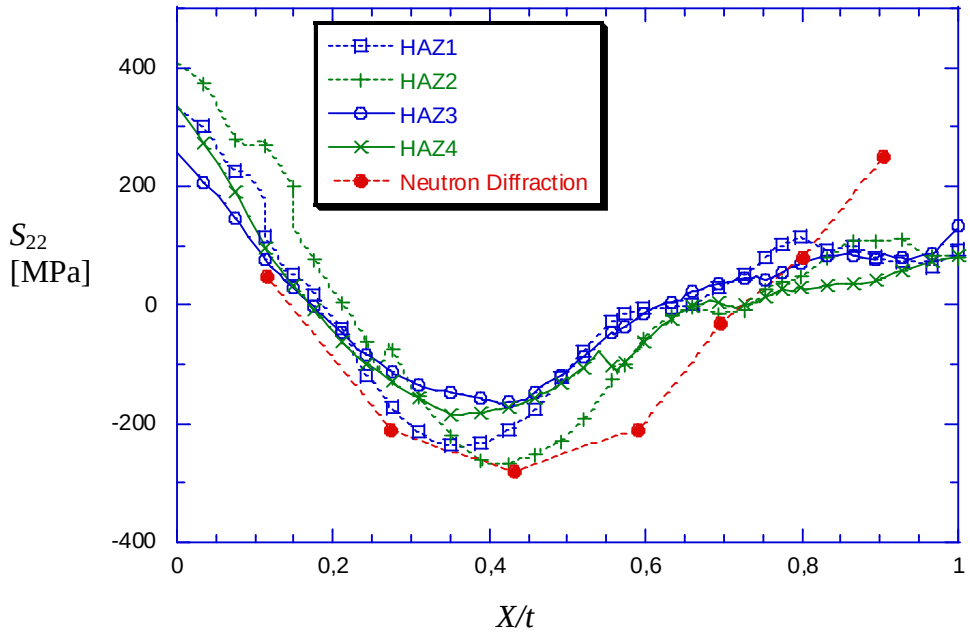

Figure 4.12: Case 2. Comparison with measurements of predicted axial residual stress (S_{22}) at 20 °C along the different HAZ paths defined in Fig. 4.8 (X/t = 0 corresponds to ID surface).

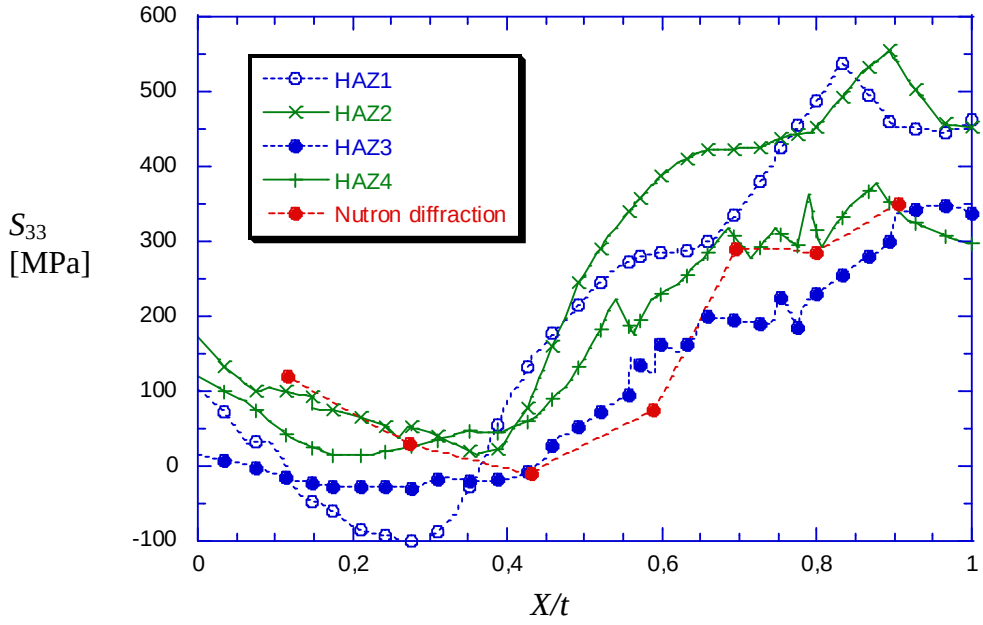

Figure 4.13: Case 2. Comparison of predicted hoop residual stress (S_{33}) at 20 °C along different HAZ paths with measurements (X/t = 0 corresponds to ID surface).

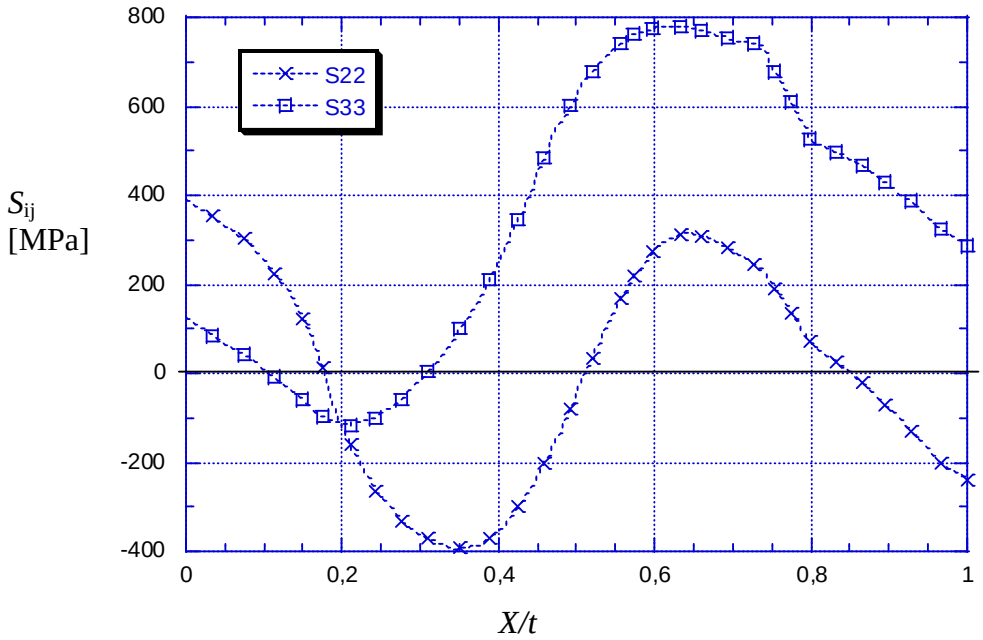

Figure 4.14: Case 2. Axial and hoop residual stresses at 20 °C along weld centre line (CL in Fig. 4.8) where X/t = 0 corresponds to ID surface.

4.3 Case 3 – Thick-walled pipe

A thick-walled pipe case having R_{in}/t = 2.8 was analysed. The geometry and the finite element mesh near the weld area are shown in Fig. 4.15. The sequence of welding (a total of 45 passes) is defined in the figure. Three through-thickness paths selected for evaluation of the detailed residual stress distributions are also indicated in Fig. 4.15, i.e. CL, HAZ, and HAZ_0.

The peak temperature during welding is shown in fig. 4.16, illustrating the predicted fusion zone and the heat affected zone shape and sizes.

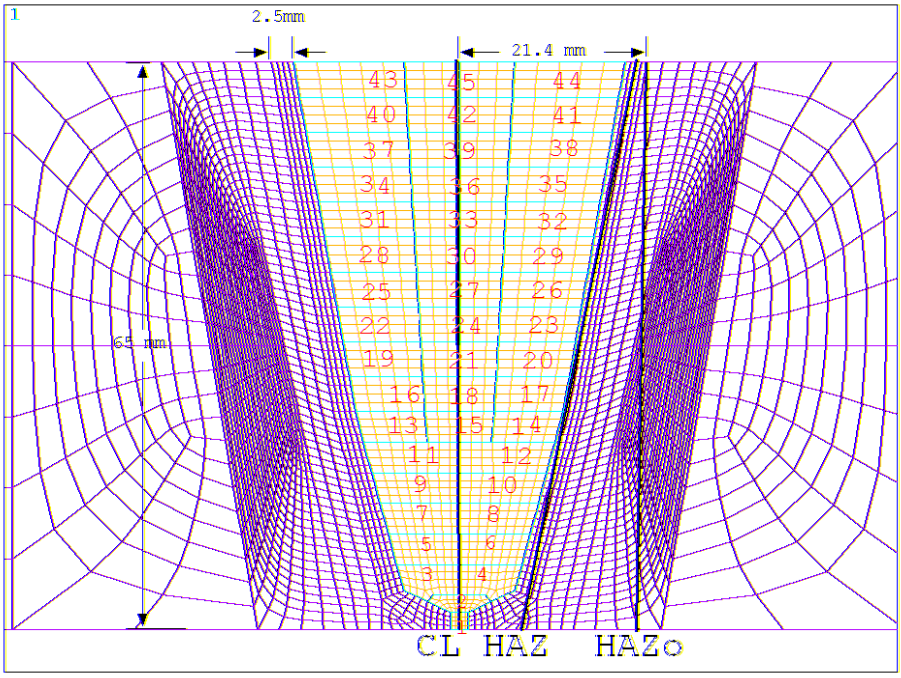

Figure 4.15: Geometry, finite element mesh and weld pass definition for Case 3.

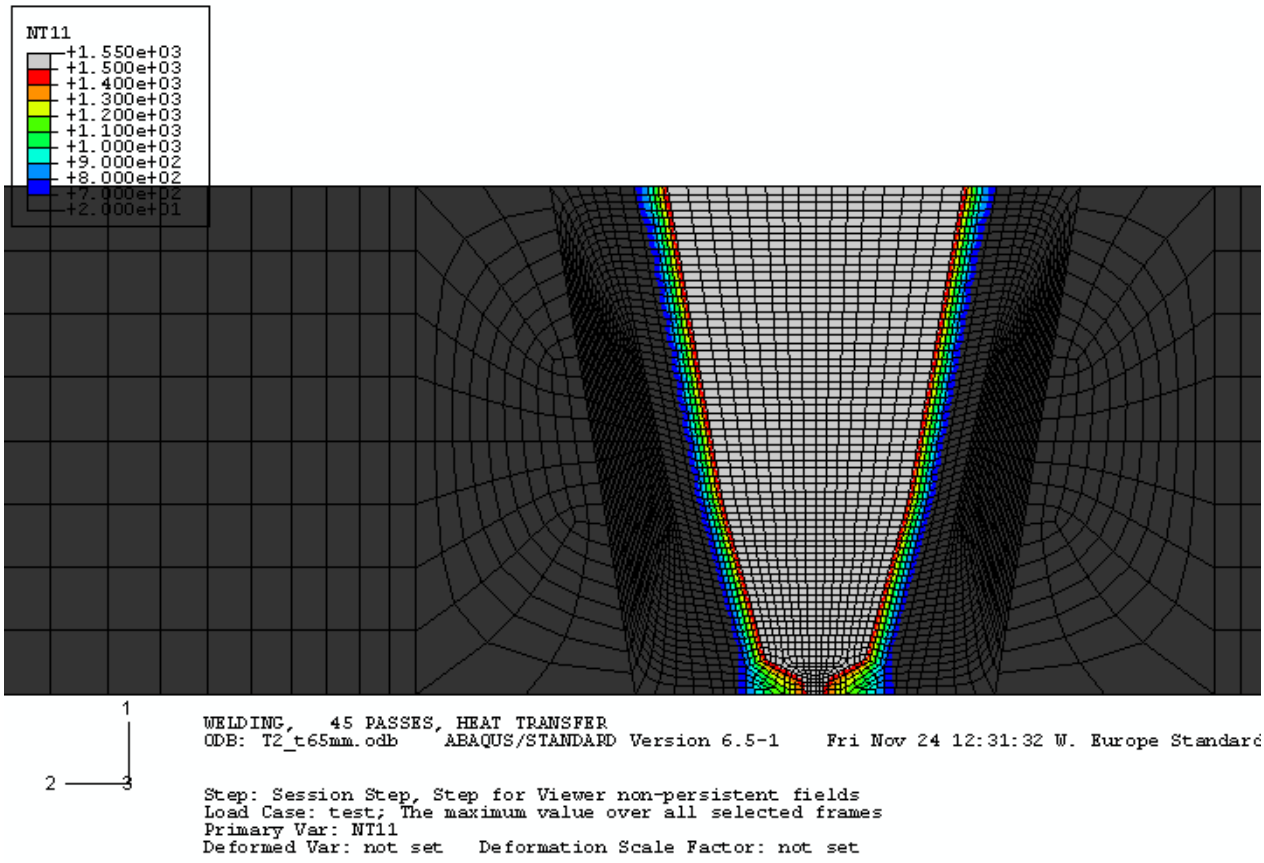

Figure 4.16: Maximum temperature experienced during the welding. The locations with a maximum temperature exceeded 1500 °C are plotted with gray colour and the locations with a maximum temperature lower than 700 °C are shown with black colour.

The final residual stress distributions at 20 °C are shown in Figs. 4.17-4.18 for the axial and hoop residual stress components, respectively. It is important to note that the axial residual stress distribution in Fig. 4.17 is significantly different from that seen in Fig. 4.4 (Case 1) and that seen in Fig. 4.10 (Case 2), although to a somewhat less degree. The axial residual stress distribution across the pipe wall thickness becomes highly localized, due to both the thick wall and small R_{in}/t ratio in Case 3. A rather similar observation can be made for the hoop residual stress distribution shown in Fig. 4.18.

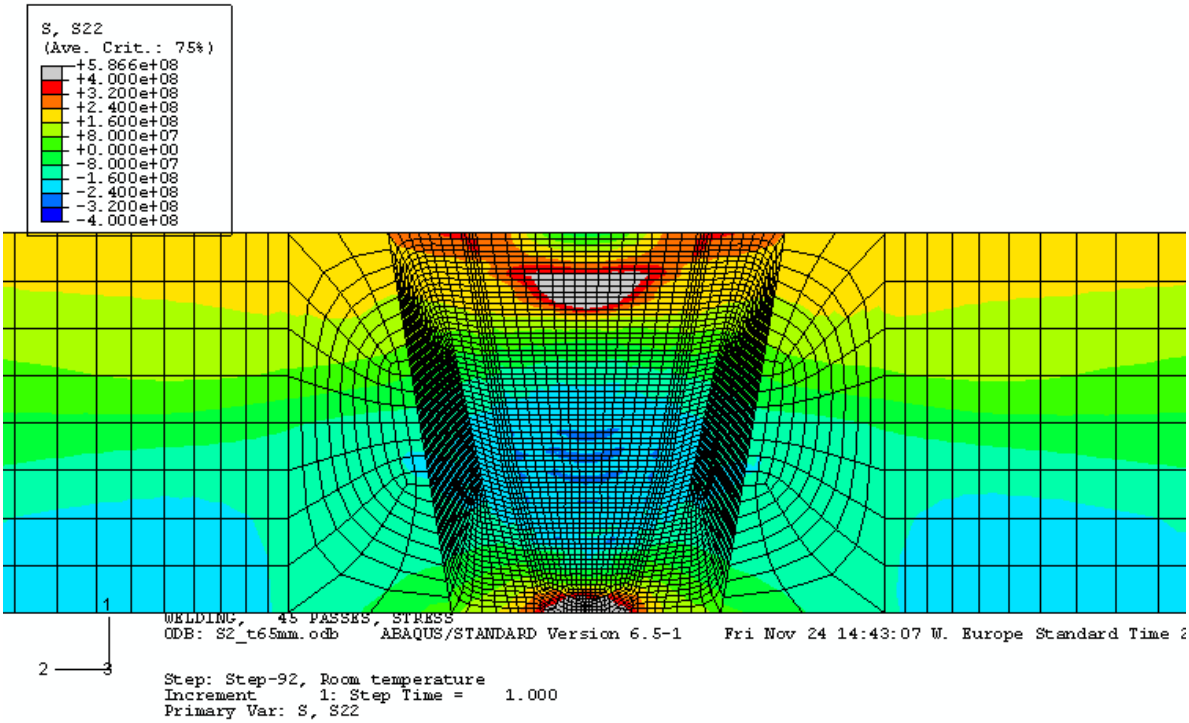

Figure 4.17: Axial residual stress for the thick-walled case 3 weld at 20 °C (unit Pa).

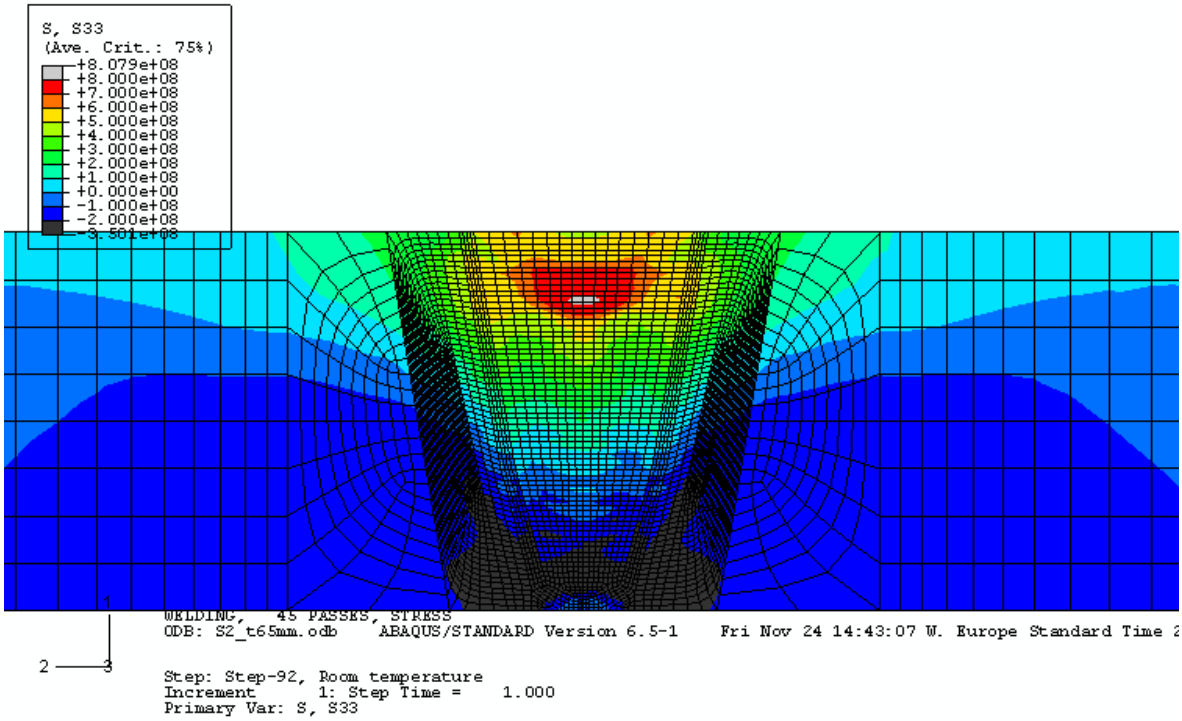

Figure 4.18: Hoop residual stress for the thick-walled case 3 weld at 20 °C (unit Pa).

The predicted residual stress distributions along the three paths (see Fig. 4.15) are compared with the available experimental measurements taken from [13] in Figs. 4.19-4.20. The surface hole measurements were taken 50mm from the weld centreline and DHD measurements were taken 20-24mm from the weld centreline. The DHD measurements were taken radially through the thickness of the pipe where holes were drilled from the outside in. The predicted axial residual stresses correlate well with the measured as shown in Fig. 4.19. The predicted hoop residual stresses are higher than the measured values around the outer diameter (OD), see Fig. 4.20.

The measured through-thickness hoop residual stress shown in Fig. 4.20 for the case using deep-hole-drilling on "Component A" is mostly compressive. Such a hoop residual stress distribution seems a little unusual if the measurement data are correct. As discussed in [4, 13], hoop residual stresses in thick pipes with small *R/t* ratio tends to show localized features, but exhibiting an overall tension due to the dominant hoop direction shrinkage deformation mode. The use of the room-temperature for inter-pass temperature, due to the lack of actual data, may have played a role in the high hoop residual stress prediction at the OD area. A further investigation of the influence is needed once additional data become available.

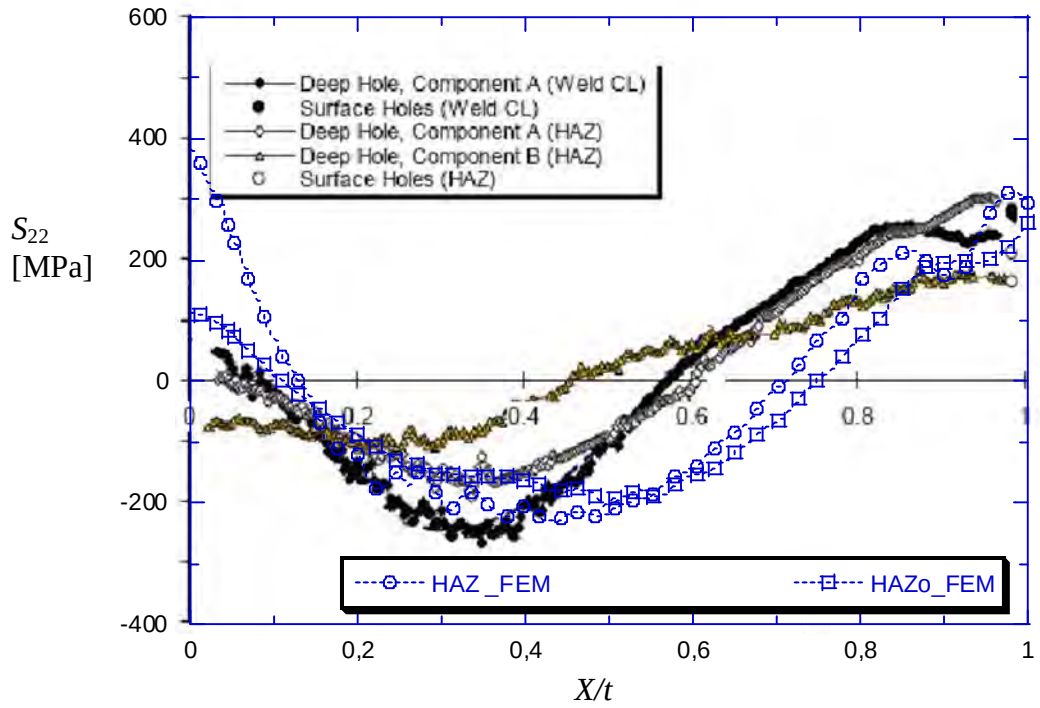

Figure 4.19: Case 3. Comparison of the predicted axial residual stress (S_{22}) at 20 °C along the different HAZ paths in Fig. 4.15 with the measured (X/t = 0 corresponds to ID surface).

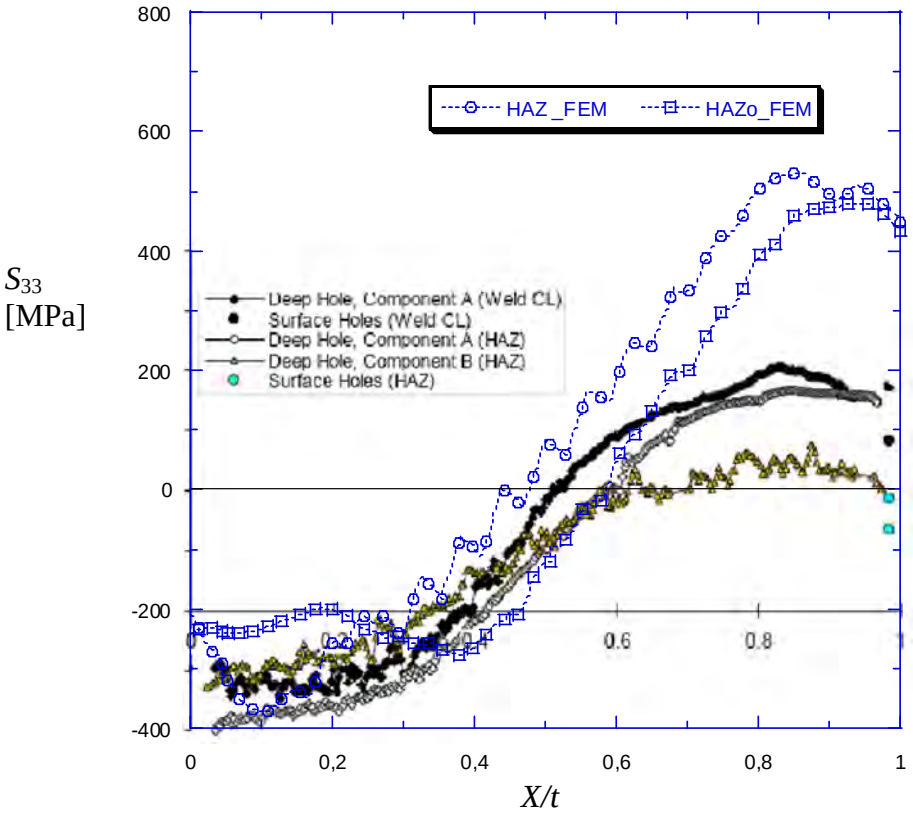

Figure 4.20: Case 3. Comparison of the predicted hoop residual stress (S_{33}) at 20 °C along the different HAZ paths in Fig. 4.15 with the measured (X/t = 0 corresponds to ID surface).

5 SENSITIVITY ANALYSES

In this section sensitivity analyses are made in order to investigate the effect of basic assumptions in the modelling. Sensitivity analyses should always be performed to assess the influence of different assumptions and parameters, especially when they are not obvious or fully elucidated and agreed upon. Efforts are made to make the residual stress predictions as realistic as possible in order to promote proper conclusions on the structural integrity. The residual stress calculations are generally based on realistic best-estimate data and assumptions, but assumptions leading to pessimistic conservative results are chosen if essential information is lacking.

Below the major new assumptions in the modelling are compared with alternative assumptions. The main important changes in the new weld residual stress modelling procedure are discussed in Section 2 and can be summarised as; (i) improved procedure for calibration of the heat source, based on analytical solutions for the HAZ size as a function of wall thickness and actual linear heat input, (ii) the use of isotropic hardening (or mixed if data is available), and (iii) the use of the annealing model for improved simulation of strain relaxation.

In references [4, 14] a number of parametric analyses on item (i) are presented, in order to demonstrate the validity of such a calibration procedure. Further investigation of heat source calibration models is not within the scope of the current project. In this section, the efforts will be focused upon the assumptions and parameters (ii) and (iii), and demonstrating their effects on the predicted residual stresses. The problem definition and conditions corresponding to Case 2 are chosen in all the subsequent sensitivity analyses.

5.1 Effect of material hardening behaviour

The weld residual stresses predicted when using isotropic hardening behaviour is compared to the stresses when assuming kinematic hardening. The annealing temperature 1200 °C is used. The residual stress distributions obtained for the different material hardening laws are presented in Figs. 5.1 - 5.4 along the paths “CL” and “HAZ1” defined in Fig. 4.8 (Case 2). It is observed that the residual stresses generated with kinematical hardening behaviour are much lower than the stresses calculated for isotropic hardening.

Included in Figs. 5.2 and 5.4 are stresses measured by neutron diffraction [32] along an HAZ path. The stress profiles and the magnitudes obtained with isotropic hardening agree well with the experimental results. Therefore it may be recommended that, if there is no experimental evidence to support the use of a kinematical hardening model, isotropic hardening should be employed in the analysis in order to generate higher stress peaks.

If detailed cyclic stress-strain material properties are available, then a mixed isotropic-kinematic hardening model could be used. Deep-hole-drilling (DHD) measurement results in Fig. 18 in [13] indicate that a mixed hardening model may result in a better agreement. The results in Fig. 5.4 also indicate that a mixed hardening model could be better. In a recent project by Ogawa et al [36] kinematic hardening was used and good agreement was obtained to the experimental data. Details of the data used in the hardening model were, however, not provided.

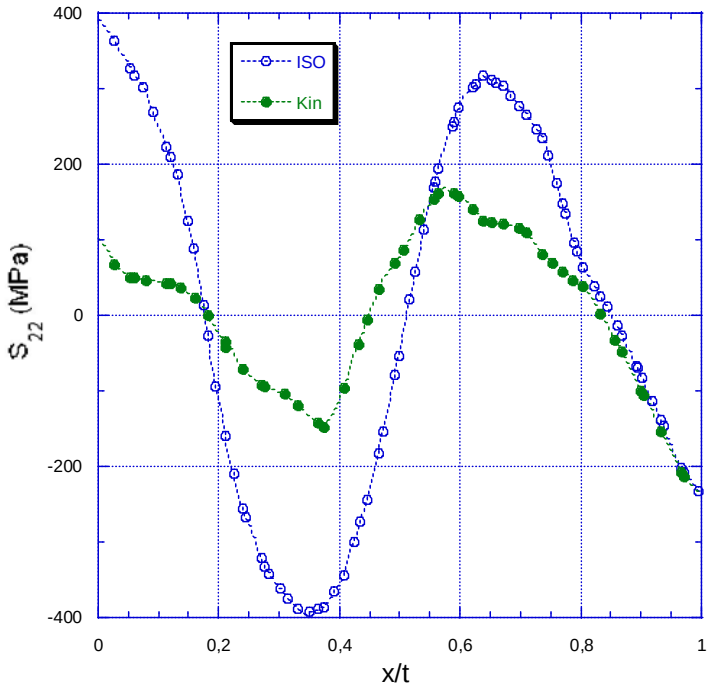

Figure 5.1: Case 2. Axial stress (S_{22}) along the weld centre line (CL) calculated using different material hardenings models (x/t = 0 corresponds to inside of the pipe).

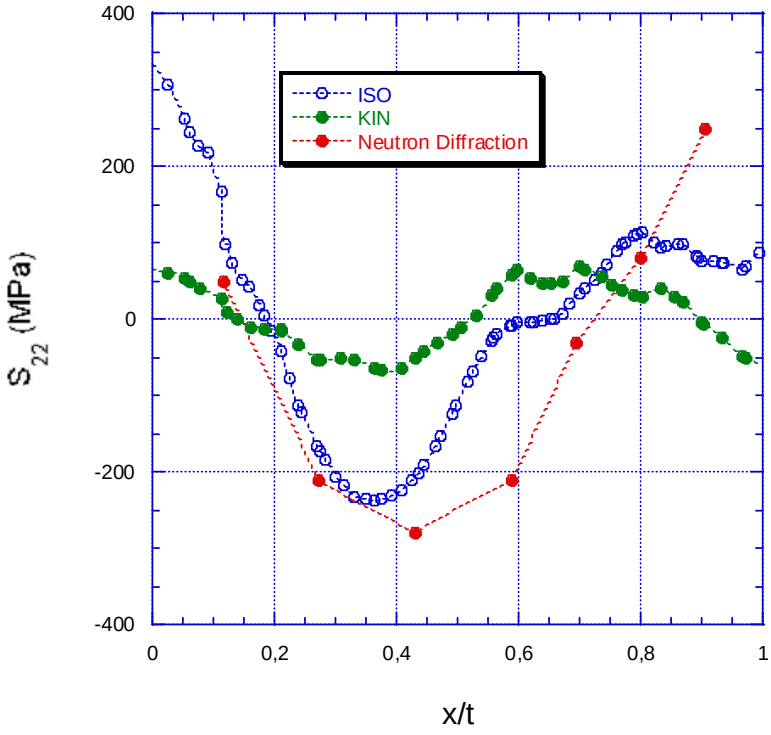

Figure 5.2: Case 2. Axial stress (S_{22}) along the path HAZ1 calculated using different material hardenings models (x/t = 0 corresponds to inside of the pipe). Stresses measured by neutron diffraction are included.

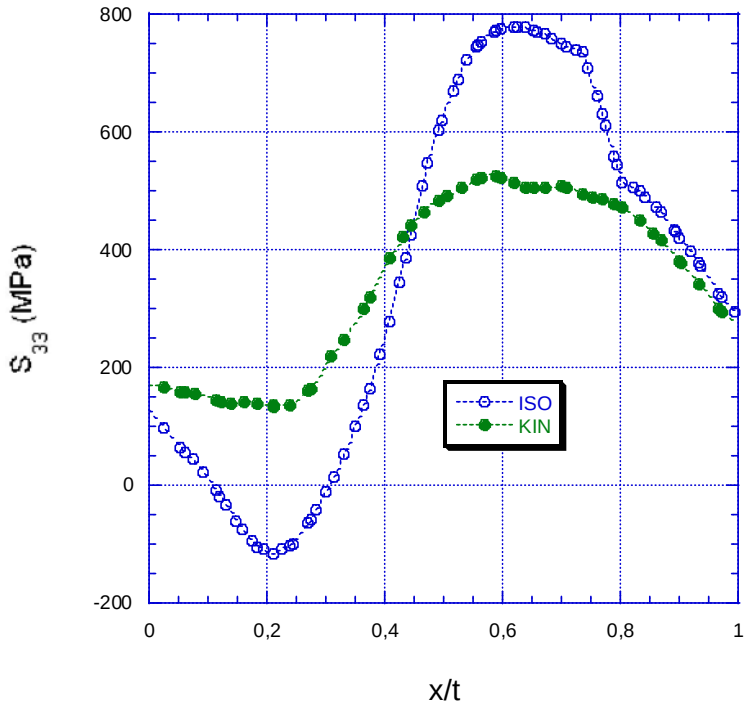

Figure 5.3: Case 2. Hoop stress (S_{33}) along the weld centre line (CL) calculated using different material hardenings models (x/t = 0 corresponds to inside of the pipe).

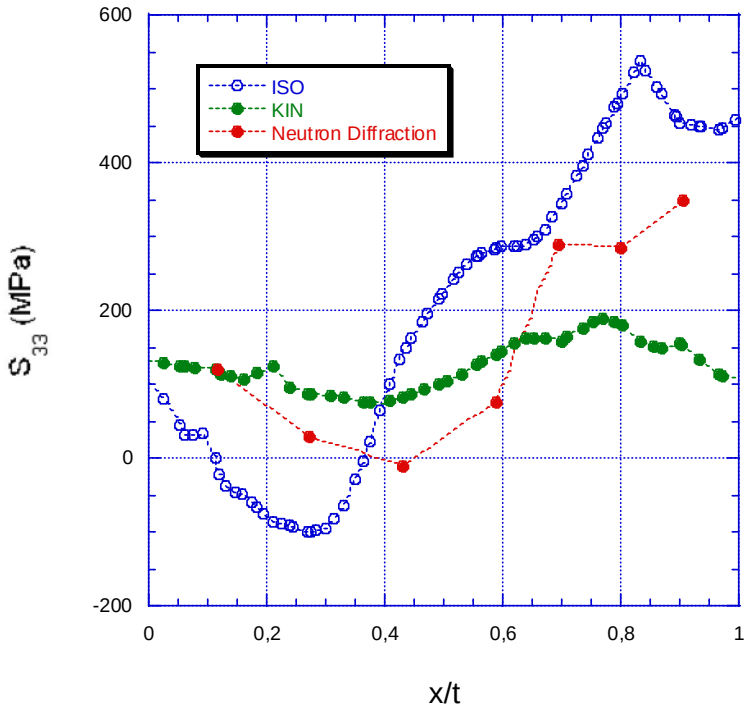

Figure 5.4: Case 2. Hoop stress (S_{33}) along the path HAZ1 calculated using different material hardenings models (x/t = 0 corresponds to inside of the pipe). Stresses measured by neutron diffraction are included.

5.2 Effect of annealing temperature

Strain relaxation due to high temperature in re-heated material is modelled by use of an annealing temperature as described in section 3.2. The choice of the annealing temperature is as discussed not obvious since the effect is not fully elucidated [15]. The effect on the predicted residual stresses from different assumed annealing temperatures is investigated below.

Figs. 5.5-5.8 shows the residual stress distributions along the paths “CL” and “HAZ1”, obtained when applying different annealing temperatures. It is seen that the annealing temperature has a strong influence especially on very high predicted residual stresses. The effect of annealing is limited for the annealing temperature 1200 °C.

“No annealing” corresponds to an infinitely high annealing temperature. In this situation, any material point going through re-melting will continue to accumulate plastic strain. Any strain-hardening behaviour considered will thus increase the residual stress magnitude. As a result, the higher the annealing temperature used, the larger the predicted residual stress magnitude becomes. Many previously publicised results were modelled without any annealing model, since this type of capability only recently became available in commercial FEA software. The lack of an annealing model was one reason that made many previous publications tend to use either elastic-perfectly plastic material model and/or kinematic material hardening law, in order to compensate for unusually high residual stress predictions. See [4] for further detailed discussion on this.

In this case a region with large influence of the annealing temperature is in HAZ at the outer diameter region where the hoop stress S33 alter by about 200 MPa for T_{anneal} changing from 1200 °C to 800 °C, see Fig 5.8. By comparing to the measured residual stress for this case, included in Fig. 5.4 (or Fig. 4.13), an anneal temperature of 800 or 1000 °C is indicated. However, a comparison for only one case can not give a clear conclusion on the anneal temperature, especially considering the experimental gauge volume and measurement scatter. Comparison should be done for a set of welds, preferably measured by several methods of latest version.

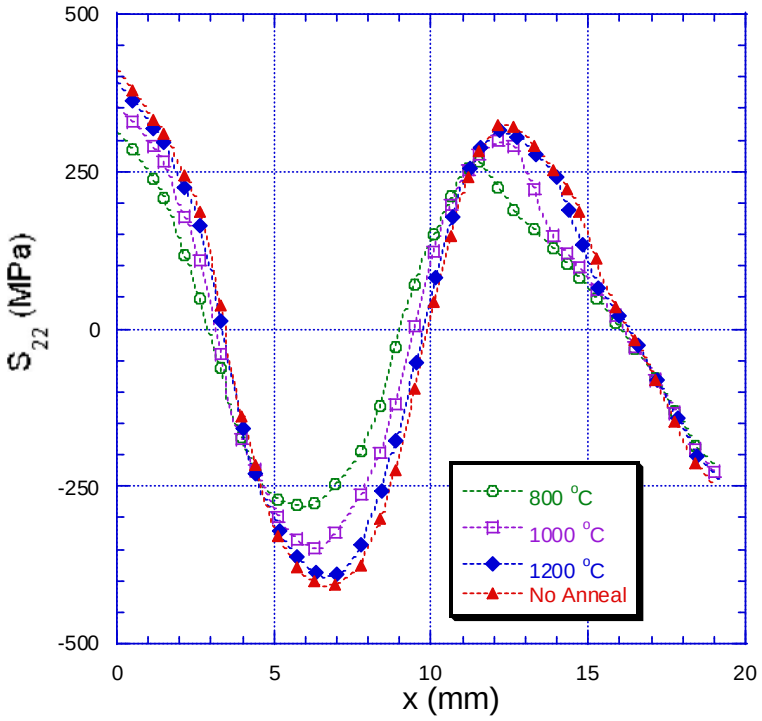

Figure 5.5: Case 2. Axial stress (S_{22}) along the weld centre line (CL) calculated using different annealing temperatures (x/t = 0 corresponds to inside of the pipe).

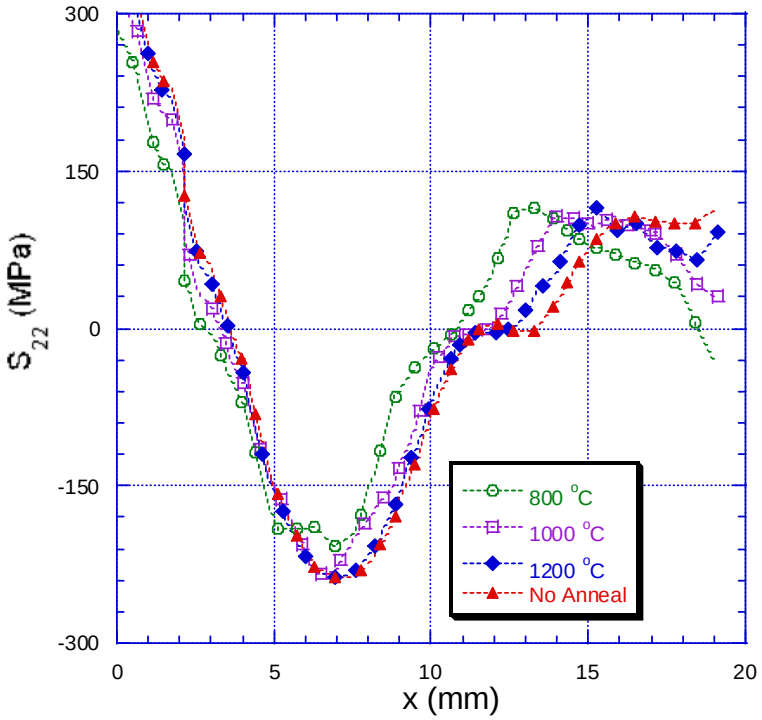

Figure 5.6: Case 2. Axial stress (S_{22}) along the path HAZ1 calculated using different annealing temperatures (x/t = 0 corresponds to inside of the pipe).

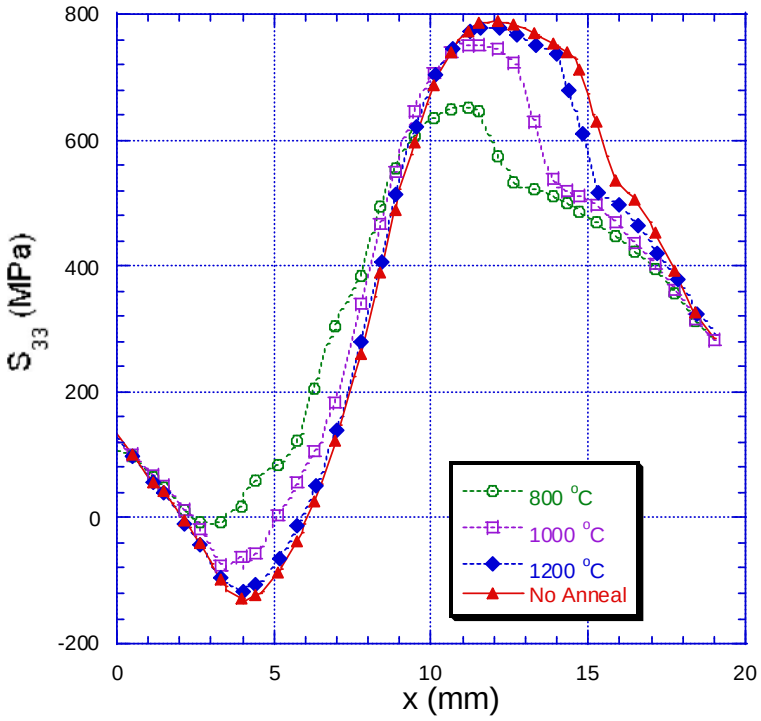

Figure 5.7: Case 2. Hoop stress (S_{33}) along the weld centre line (CL) calculated using different annealing temperatures (x/t = 0 corresponds to inside of the pipe).

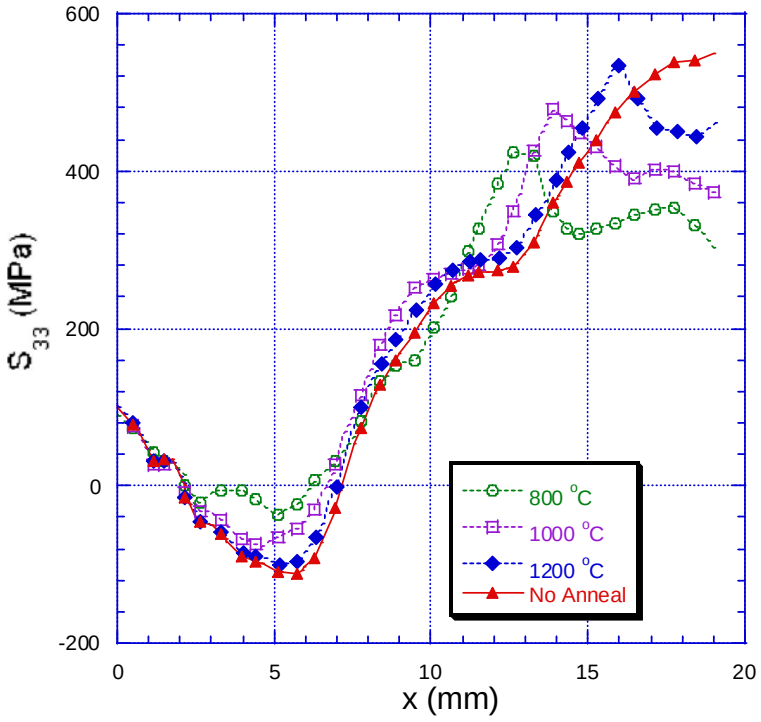

Figure 5.8: Case 2. Hoop stress (S_{33}) along the path HAZ1 calculated using different annealing temperatures (x/t = 0 corresponds to inside of the pipe).

6 COMPARISON OF NEW AND PREVIOUS STRESS PREDICTIONS

In this section results predicted by the new and the earlier residual stress modelling procedures are compared. A medium thick-walled pipe is considered, the Case 2. As discussed in Section 2, the major differences between the two modelling procedures are (i) the improved procedure for calibration of the heat source, (ii) the use of isotropic hardening, and (iii) the use of an annealing model.

Figs. 6.1-6.4 highlight the large difference in the predicted residual stresses between the new and old modelling procedures. In this chapter, 'old' denotes the use of the old heat calibration method, kinematic hardening and no annealing; 'new' denotes the use of the new heat calibration method, isotropic hardening and an annealing temperature of 1200ºC.

6.1 Axial residual stresses

As shown in Fig. 6.1, the axial residual stress distribution along the weld centreline (CL) predicted using the new procedure is significantly different from the one predicted using the earlier procedure. The result from the new procedure shows a strong through-thickness variation, typically seen in recent investigations by simulations and measurements for intermediate thickness pipes with multiple passes (small relative bead size). The earlier procedure predicts an almost linear distribution from ID surface to OD, which is normally seen in much thinner pipes and for larger *R/t* ratios.

The validation to experimental neutron diffraction results along HAZ, shown in Fig. 6.2, clearly demonstrate that the new procedure results in a large improvement of the accuracy of the predicted through-thickness stress profile.

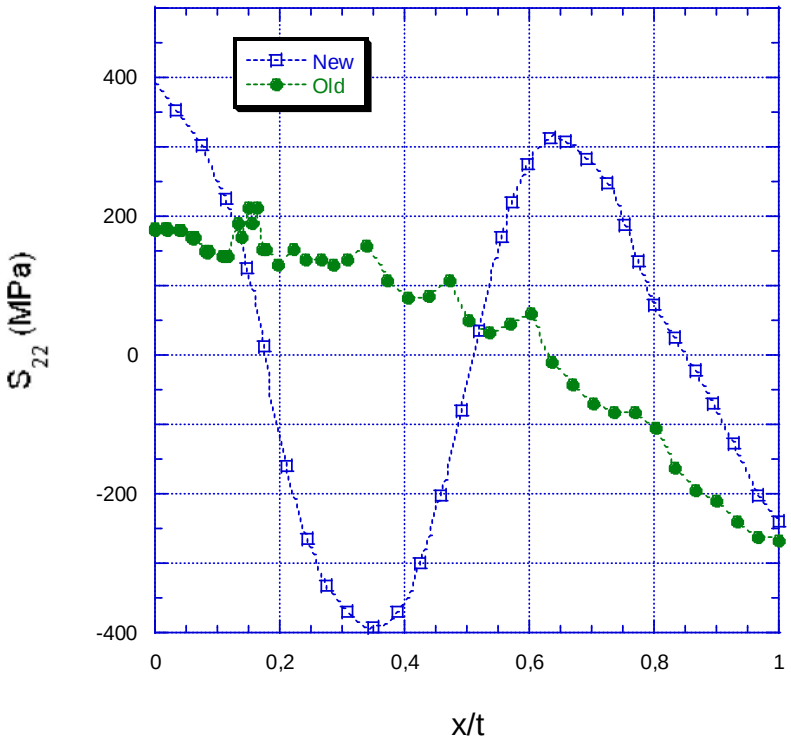

Figure 6.1: Comparison of axial weld residual stress along the weld centre line (CL) in case 2, predicted by the new and old modelling procedures (x/t = 0 at pipe inside).

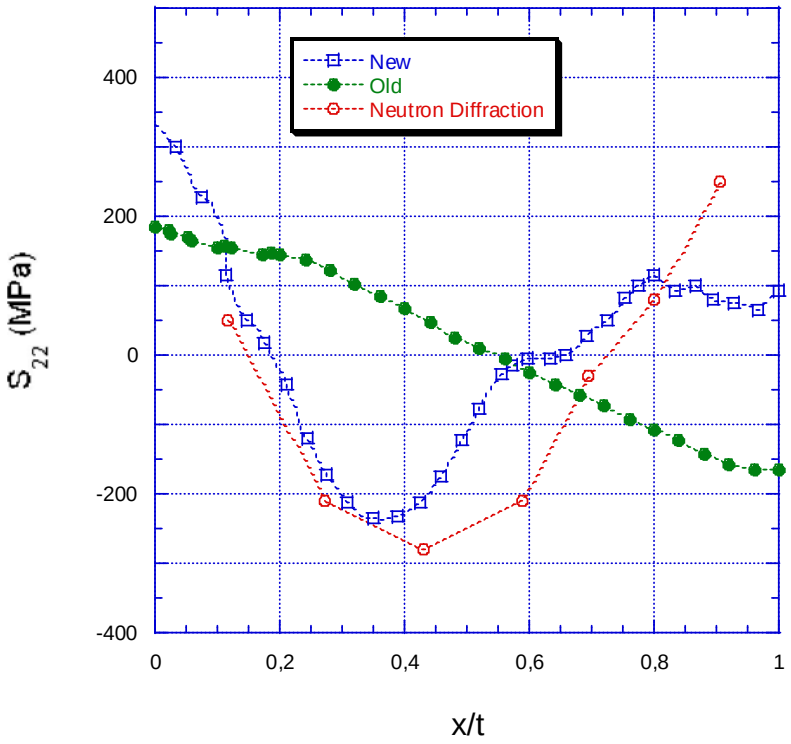

Figure 6.2: Comparison of axial weld residual stress along the path HAZ1 in case 2, predicted by the new and old modelling procedures (x/t = 0 at pipe inside).

If the improved heat source calibration procedure (which generally reduces heating) was introduced solely, and kinematic hardening still used, the difference is indicated by the results in Fig. 5.1-5.4. This shows that the improvement of the heat source model and calibration method had a dramatic effect on prediction of the weld induced residual stress.

6.2 Hoop residual stresses

Figs. 6.3-6.4 compare the predicted hoop residual stresses along weld centreline (CL) for the new and the earlier modelling procedure. A similar trend as discussed in Section 6.1 is observed for this stress component as well.

The validation to experimental measurement data along HAZ in Fig. 6.4 supports the predictions using the new procedure, at least in trend.

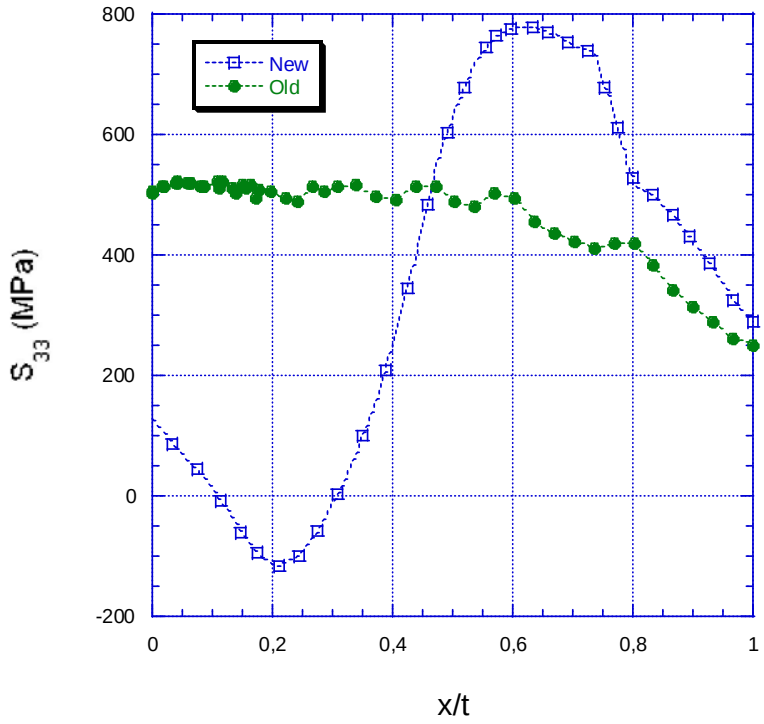

Figure 6.3: Comparison of hoop weld residual stress along the weld centre line (CL) in case 2, predicted by the new and old modelling procedures (x/t = 0 at pipe inside).

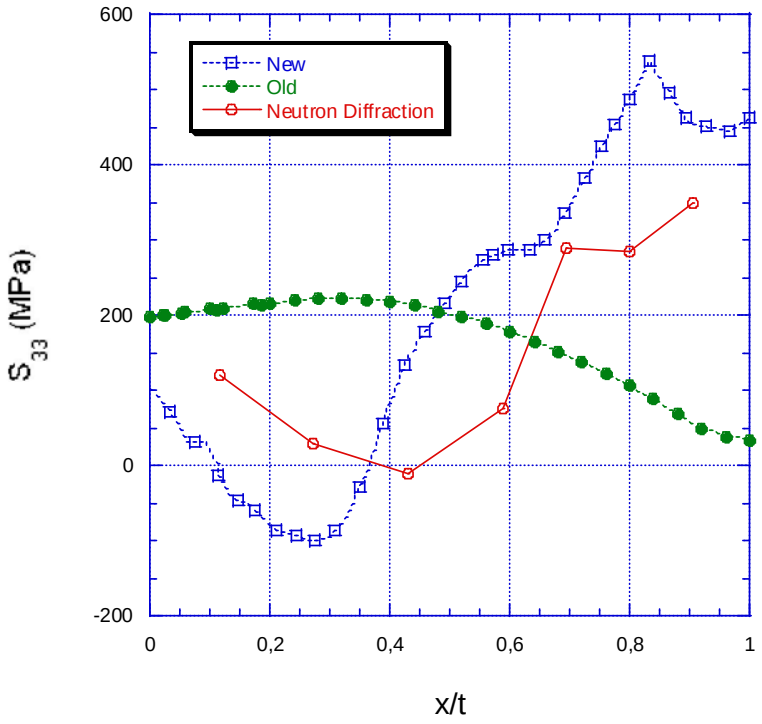

Figure 6.4: Comparison of hoop weld residual stress along the path HAZ1 in case 2, predicted by the new and old modelling procedures (x/t = 0 at pipe inside).

7 DISCUSSION AND RECOMMENDATIONS FOR FUTURE WORK

Any engineering model has to be validated to experiments and measurements in order to demonstrate that its output is representative for the reality. Weld residual stress calculation models are complex and involve several physical processes and accompanying assumptions, and is of course no exception from this need for verification. Efforts are made to make the weld residual stress predictions as realistic as possible, and avoid pessimistic conservative assumptions, in order to promote proper conclusions on the structural integrity. This will help achieving effective measures and requirements that ensure safe operation. The residual stress calculations are generally based on realistic best-estimate data and assumptions, if the essential information is available. This also puts requirements to analyse any remaining issues and demonstrate the accuracy of weld residual stress models.

Large improvements have been made by the new weld residual stress modelling procedure developed in this project. However, there still exist some questions that are not fully resolved. As discussed above, well grounded assumptions are fundamental in order to attain a reliable prediction model. Some issues in weld residual stress modelling still needs further investigation in order to confirm and settle some basic assumptions and approximations. Further model refinements should preferably be validated to residual stress fields measured using the latest versions of the measuring methods.

7.1 Recommendations for future work

Below larger issues that still remain within weld residual stress modelling are listed. For each identified issue a tangible proposal is given for how to solve the problem.

1) **Further development and validation of heat source calibration procedure.**
   The heat source calibration procedure has a major influence on the resulting stresses, and further development and verification of the calibration models is recommended.

   The model proposed in this report is based on calibration by use of an analytical solution for the HAZ size, as a function of wall thickness, material, actual weld speed and linear heat input. This is a major step forward. However, during the project a few ideas on further improvements of the method have been identified. Work is required to identify the best method for hold time calibration when adapting the 3D heat source model solution to a 2D welding simulation. Additionally, it must be confirmed that the 'HAZ width' is the best metric for describing equivalence of heat transfer between 3D and 2D welding models.

   In order to get an even better relation between the linear heat input and the size of the fusion zone (and the gradient to HAZ), a further natural improvement to the current procedure would be to develop a Gaussian distribution heat source solution.

2) **Sensitivity analysis using best-estimate yield strength data for 316.**
   The weld residual stress calculation in this project was performed assuming standard general material data for austenitic stainless steel. A closer review of the general stainless steel data according to [6, 7] was made towards the end of this project. According to ASME SA-240, the steel 316L and 304L has the same minimum required yield strength, 170 MPa at 20 °C. The general data for austenitic stainless steel in [6, 7] corresponds to 304 steel. However, when reviewing typical measured data for these steels, it was revealed that they differ and the 316L steel shows up to about 50% higher yield stress values for unstrained material. In order to avoid underestimation of the residual stress, best-estimate yield data should be used in weld

residual stress calculations. Because of this a sensitivity analysis using typical 316L data is proposed.

3) **Use of virgin-state weld material properties**.
It is common to use weld metal properties measured for as-welded material, with the argument to be conservative. In this project also, separate data were used for the austenitic base and weld material, according to [6, 7]. In order to get accurate predictions of the residual stress it is however proposed that the virgin state yield properties of the filler material is used. This is more correct since the simulation model includes the generation of plastic strains, which will result in the hardening of the weld material.

Recent measurements of the local yield stress in welds [35, 15], show that the weld material plastic properties, in as-welded condition, typically corresponds to a plastic strains of the order of 5 - 10%. This corresponds well to typical strain obtained in welding simulations. Thus, the use of virgin non-welded filler material properties (or corresponding base material properties) should increase the accuracy obtained in modern welding models.

An analysis is proposed where virgin-state weld material properties and as-welded properties, are applied and compared to experimental data in order to verify if the agreement is improved.

4) **Effect of mixed isotropic-kinematic hardening model**
Detailed cyclic stress-strain material properties are now available for 316 austenitic steel. It is proposed that a study is performed to evaluate the result from using a mixed isotropic-kinematic hardening model (expanding and translating yield surface). The results should be compared to isotropic and kinematic hardening results, in order to assess the accuracy and realism in the proposed use of isotropic hardening as a standard model.

5) **Settle the anneal temperature for weld residual stress simulations.**
Unrealistic plastic strain may accumulate in areas close to the fusion line and in the HAZ, which affect the final residual stress results, especially in the HAZ. Weld and base material adjacent to a new weld bead will reach high temperatures or even re-melt, and the resulting strain relaxation, and the new strain free temperature, in these regions should be modelled in detail.

As demonstrated in this work, the use of an annealing model can influence the residual stress field considerably. The anneal temperature can simulate rapid strain relaxation at high temperatures in re-heated material. Arguments and recommendations for what anneal temperature (or transition region) to use are however lacking. Data for the rate of recrystallization or creep at high temperatures is rare, and it has been argued for the use of an “anneal temperature“ in the range 900 - 1200 °C. It is however necessary to demonstrate that these assumptions are well founded, and in order to establish the actual annealing temperature to use further work is required.

It is recommended to develop simple estimates of the rate of recrystallization and creep at high temperatures (in austentic material) from a literature survey. In relation to the effective time at high temperatures, and the dominating process for strain relaxation, a rationale for the choice of the anneal temperature can be developed. In addition to the strain relaxation in material heated to high temperatures, also the effect of resetting the new strain free temperature in these regions should be evaluated. The proposed anneal temperature can be validated to experiments

by analysis of a set of well documented weld geometries that covers a wide range of pipe geometries and types of residual stress fields. Since measurements methods has improving rapidly, as new measurements as possible should be used for the comparisons.

8 CONCLUSIONS

The objective of this work is to identify and evaluate improvements to the existing residual stress modelling procedure used in Sweden. The study was focused on the development and validation of an improved weld residual stress modelling procedure, by taking advantage of the recent advances in residual stress modelling and stress measurement techniques.

The earlier procedure used by Inspecta has provided adequate baseline residual stress information, through an appropriate interpretation for achieving conservative fracture mechanics assessments. However, there is a growing demand to eliminate any unnecessary conservatism involved in residual stress assumptions. Efforts are made to make the weld residual stress predictions as realistic as possible, and avoid pessimistic assumptions, in order to promote proper conclusions from subsequent fracture assessments. This will help achieving effective measures and requirements that ensure safe operation of nuclear power plants.

Modelling and measurement techniques have evolved since the earlier procedure was first put in place more than a decade ago. Weld residual stress modelling procedures can be rather complex due to the multi-physics and multi-scale nature involved in welding processes. The project team consisting of engineers from Inspecta and Battelle has however focused upon identifying and implementing the most relevant modelling procedures, which have been proven essential and effective.

The main improvements in the new weld residual stress modelling procedure can be summarised as:

1) Improved procedure for heat source calibration. The new calibration procedure is based on use of analytical solutions for the HAZ size, as a function of wall thickness, material, actual weld speed and linear heat input. This will reduce the risk of overheating, especially when actual linear heat input is used in axi-symmetric models.
2) Use of isotropic hardening model as standard. Experience from recent comparisons to measured weld residual stress fields indicates that the stress profiles are better captured using isotropic hardening. If detailed cyclic stress-strain material properties are available, then a mixed isotropic-kinematic hardening model could be used.
3) Use of an anneal modelling for improved simulation of rapid strain relaxation at high temperatures in re-heated material.

The new modelling procedure is demonstrated to capture the main characteristics of the through-thickness stress distributions by validation to experimental measurements. Three austenitic stainless steel butt-welds cases are analysed, covering a large range of pipe geometries. From the cases considered it is evident that there can be large differences between the residual stress predicted using the new procedure, and the earlier procedure or handbook recommendations. The stress profiles according to the new procedure agree well with the measured data. Residual stress predicted by the new procedure is more accurate while achieving a reasonable conservatism.

9 REFERENCES

1. SKIFS 2005:2, "*Regulation on mechanical devices in nuclear facilities*", The Swedish Nuclear Power Inspectorate's Regulatory Code, SKI, 2005.
2. Brickstad, B. *et al*, "*Procedure used in Sweden for safety assessment of components with cracks*", Int. J. of Pressure Vessels and Piping, Vol. 77, pp. 877-881, 2000.
3. Dillström P. *et al.*,"*Handbook — A combined deterministic and probabilistic procedure for safety assessment of components with cracks*", DNV RSE Report No 2004/01 Rev 4-1, Det Norske Veritas AB, DNV Technology Sweden, 2004.
4. Dong, P. and Hong, J.K., "*Recommendations on Residual Stress Estimate for Fitness-for-Service Assessment*", WRC Bulletin, No. 476, 2003.
5. Dong, P., "*Length Scale of Secondary Stresses in Fracture and Fatigue*", Int. J. of Pressure Vessels and Piping, Vol. 85, p. 118-117, 2008.
6. Brickstad B, and Josefson L, "*A parametric study of residual stresses in multi-pass butt-welded stainless steel pipes*", Int. J. Pressure Vessels and Piping, Vol. 75, p.11–25, 1998.
7. Delfin P, Bricksatd B, and Josefson L, "*Residual stresses in multi-pass butt-welded bi-metallic piping, part I*", SAQ/FoU-Report 98/12, SAQ Kontroll AB. 1998.
8. Delfin P, Brickstad B, and Gunnars J, "*Residual stresses in multi-pass butt-welded bi-metallic piping, part II*", SAQ/FoU-Report 99/06, SAQ Kontroll AB, 1999.
9. Dong, P. and Brust, F.W, "*Welding Residual Stresses and Effects on Fracture in Pressure Vessel and Piping Components: A Millennium Review and Beyond*", The Millennium Issue, ASME Transactions: Journal of Pressure Vessel Technology, Vol. 122, No. 3, August 2000, pp. 329-328.
10. Dong, P. and Hong, J.K., "*Fracture Mechanics Treatment of Residual Stresses in Defect Assessment*", *Welding in the World*, Vol. 48, pp. 28-38, 2004.
11. Borjesson, L., Lindgren, L-E, "*Simulation of Multipass Welding With Simultaneous Computation of Material Properties*", J. Engng Materials and Technology, Vol. 123, p. 106-111, 2001.
12. Hansen, J. L., "*Numerical Modelling of Welding Induced Stresses*", Ph.D. thesis, Department of Manufacturing Engineering and Management, Technical University of Denmark, ISBN 87-90855-52-3, 2003.
13. Bouchard, P.J., "*Validated residual stress profiles for fracture assessments of stainless steel pipe girth welds*", Int. J. Pressure Vessels & Piping, Vol. 84, p. 195–222, 2007.
14. Dong, P. *et al., "JIP on Residual Stress Estimate and Post-Weld Heat Treatment"*, Pressure Vessel Research Council (PVRC), 2002-2005.
15. L. Edwards, *et al., "Advances in Residual Stress Modeling and Measurement for the Structural Integrity Assessment of Welded Thermal Power Plant"*, Advanced Materials Research, Vols. 41-42, p. 391-400, 2008.
16. Smith, D.J., Bonner, N.W., "*Measurement of residual stress using the deep hole method*", Proc. of Int. Conf on Residual Stresses in Design, Fabrication, Assessment and Repair, ASME PVP-Vol 327, p. 53-65, 1996.

17. Smith, D.J., Bouchard, P.J., George, D., *"Measurement and prediction of residual stresses in thick-section steel welds"*, J. Strain Analysis for Engineering Design, Vol. 35, p 287-305, 2000.

18. R.V. Martins and V. Honkimäki, *"Depth Resolved Investigation of Friction Stir Welds Made from AA2024 / AA2024 and AA2024 / AA6082 Using a Spiral Slit and High Energy Synchrotron Radiation"*, Materials Science Forum, Vols. 490-491, p. 424-429, 2005.

19. B. Hasse, M. Koçak and W. Reimers, *"Determination of residual stress fields with high local resolution"*, Materials Science Forum, Vols. 524-525, p. 279-28, 2006.

20. Withers P.J. and Bhadeshia H.K.D.H.,*"Residual stress. Part 1 – Measurement techniques"*, Mat. Sci and Techn, Vol 17, p. 355-365, 2001.

21. Withers P.J., "*Mapping residual and internal stress in materials by neutron diffraction*", Comptes Rendus Physique, Volume 8, Pages 806-820, 2007.

22. Price J.W.H., Ziara-Paradowska A.M, Joshi S., Finlayson T., C Semetay C., Nied H., "*Comparison of experimental and theoretical residual stresses in welds: The issue of gauge volume"*, Int. J. Mechanical Sciences, Vol. 50, pp. 513-521, 2008.

23. M. Kartal, *et al., "Residual stress measurements in single and multi-pass groove weld specimens using neutron diffraction and the contour method"*, Materials Science Forum, Vols. 524-525, p. 671-676, 2006.

24. M.B. Prime, *et al., "Laser Surface-Contouring and Spline Data-Smoothing for Residual-Stress Measurement, Experimental Mechanics"*, Vol. 44, p. 176-184, 2004.

25. Withers P.J., *et al., "Recent advances in residual stress measurement"*, Int. J. Pressure Vessels and Piping, Vol. 85, p.118-127, 2008.

26. *ABAQUS User's manual*, Version 6.5, 2005.

27. Rosenthal, D., *"Mathematical theory of heat distribution during welding and cutting"*, Welding Journal, Vol. 20, p. 220-234, 1941.

28. Friedman, E., *"Thermomechanical Analysis of the Welding Process using the Finite Element Method"*, Journal of Pressure Vessel Technology, Trans. ASME, Vol. 97, p.206-213, 1975.

29. Goldak, J., Chakravarti, A. and Bibby, M., *"A New Finite Element Model for Welding Heat Sources"*, Met. Trans. B, Vol. 15B, p. 299-305, 1984,

30. Taylor, G.A. *et al., "Finite volume methods applied to the computational modelling of welding phenomena"*, Proceedings of Int. Conf. on CFD in the Minerals and Process Industries, CSIRO, Melbourne, Australia, 1999.

31. Eagar, T.W. and Tsai, N.-S., *"Temperature Fields Produced by Traveling Distributed Heat Sources"*, Welding Research Supplement, p. 346-355, 1983.

32. L. Edwards, G. Bruno, M. Dutta, P.J. Bouchard, K.L. Abbott and R. Lin Peng, "*Validation of Residual Stress Predictions for a 19 mm thick J-preparation Stainless Steel Pipe Girth Weld using Neutron Diffraction"*, Proc. Sixth International Conference on Residual Stresses, ICRS6, p. 1523-1526, Oxford University, Institute of Materials, UK, 2000.

33. S.K. Bate, P.J. Bouchard, P.J. Flewitt, D. George, R.H. Leggatt and A.G. Youtsos, "*Measurement and Modelling of Residual Stress in Thick Section Type 316 Stainless Steel Welds"*, Proc. Sixth International Conference on Residual Stresses, ICRS6, p. 1511-1518, Oxford University, Institute of Materials, UK, 2000.

34. Dong, P., “Residual Stress Analysis of a Multi-Pass Girth Weld: 3D Special Shell Versus Axisymmetric Models,” *Journal of Pressure Vessel Technology*, Vol. 123, p 207-213, 2001.

35. M. Kartal, *et al*., *”Determination of Weld Metal Mechanical Properties Utilising Novel Tensile Testing Methods”*, Applied Mechanics and Materials, Vols. 7-8, p. 127-132, 2007.

36. K. Ogawa, E.J. Kingston, D.J. Smith, T. Saito, R. Sumiya, Y. Okuda, “The measurement and modelling of residual stresses in a full-scale BWR shroud-support mock-up”, Proceedings of PVP2008 – 2008 ASME Pressure Vessels and Piping Division Conference, Chicago, PVP2008-61548, 2008.

37. Material specification, **Specs: 304**, Sandmeyer Steel Company, 2008.

38. PJ Bouchard, MT Hutchings and PJ Withers, “Charactersiation of the residual stress state in a double ‘V’ stainless steel cylindrical weldment using neutron diffraction and finite element simulation”, Proc. Sixth International Conference on Residual Stresses, ICRS6, p. 1333-1340.

APPENDIX 1 – MECHANICAL AND THERMAL MATERIAL PROPERTIES

Mechanical material parameters used in the new weld residual stress modelling procedure, for the weld and parent material, are listed in Table A1.

Table A1 Mechanical properties for stainless steel (304) and weld [6,7, 37].

Temperature [^{o}C]	**Young's modulus *E* [GPa]**	**Poisson's ratio [-]**	**Yield stress (304) [MPa]**	**Yield stress (Weld) [MPa]**
20	200	0.3	216	460
100	195	0.3	173	419
200	185	0.3	140	368
400	170	0.3	116	264
600	155	0.3	85	210
800	145	0.3	70	154
1000	96	0.3	50	50
1200	50	0.3	10	10
1340	10	0.3	10	10
1390		0.3	10	10

A bilinear hardening model was used in the new weld residual stress modelling procedure, as discussed in Section 3.2. The model, illustrated in Fig. A1, is described by,

$\sigma_f = \sigma_y + K\varepsilon^{pl}$ *where* $0 \le \varepsilon^{pl} \le \varepsilon_0$, and

$\sigma_f = \sigma_0$ *where* $\varepsilon^{pl} > \varepsilon_0$ (A1)

where σ_f, σ_y and ε^{pl} are the flow stress, yield stress and equivalent plastic strain, respectively and σ_0, ε_0 and K are material parameters. A value of 0.1 was assigned to ε_0.

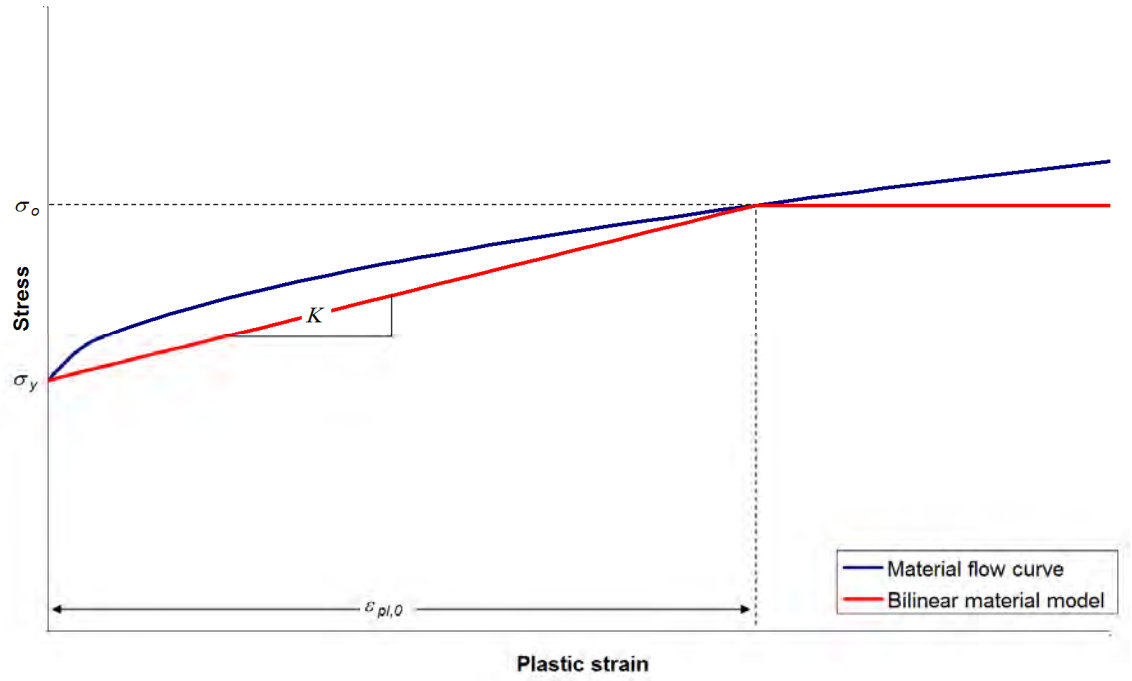

Figure A1: Illustration of the bilinear hardening model (in red) used in the new weld residual stress modelling procedure. Parameters for the model were obtained by fitting to an experimentally determined material flow curve (illustrated in blue).

Thermal material parameters used in the new weld residual stress modelling procedure, for the weld and parent material, are listed in Table A2.

Table A2 Thermal properties for stainless steel (304) [6,7, 37].

Temperature [^{o}C]	**Conductivity [W/m/^{o}C]**	**Specific heat [J/kg/^{o}C]**	**Thermal expansion [10^{-6}/^{o}C]**
20	15.0	442	17.0
100	15.5	479	17.0
200	17.5	515	17.5
300	18.8	539	18.0
400	20.0	563	18.5
500	21.3	572	18.75
600	22.5	581	19.0
800	24.0	596	19.5
1000	25.5	609	20.0
1200			20.0
1340			20.0
1390			20.0

Strålsäkerhetsmyndigheten
Swedish Radiation Safety Authority

SE-171 16 Stockholm
Solna strandväg 96

Tel: +46 8 799 40 00
Fax: +46 8 799 40 10

E-mail: registrator@ssm.se
Web: stralsakerhetsmyndigheten.se